ABSTRACT

Title of Thesis:	RESOLUTION OF PM SOURCES USING HIGHLY TIME RESOLVED DATA AND DISCRETE PARTICLE SIZE BINS
	Melissa Rury, Master of Science, 2006
Directed By:	Dr. John Ondov, Department of Chemistry and Biochemistry

The goal of this project was to explore the use of particle size distribution data for distinguishing between local vs distant and controlled vs uncontrolled combustion sources. A two day period in July was selected for an apportionment study from eleven months of highly time resolved data collected at the Baltimore Supersite. Number concentration vs particle size data was partitioned into four size bins as follows: a nucleation mode (<80 nm), fresh combustion (80-300 nm), secondary aerosol (0.3-1 µm), and coarse particles (1-2.5 µm).

Two multivariate receptor model studies were completed using positive matrix factorization. The first model included size binned particle counts, the second, included binned particle mass concentrations. Using this combination of models, we identified eight factors. Three sources were identified by both model results, while additional sources not identified by number concentrations were identified when we applied the mass moments to weight the size distribution data.

RESOLUTION OF PM SOURCES USING HIGHLY-TIME RESOLVED DATA
AND DISCRETE PARTICLE SIZE BINS

By

Melissa A. Rury

Thesis submitted to the Faculty of the Graduate School of the
University of Maryland, College Park, in partial fulfillment
of the requirements for the degree of
Master of Science
2006

Advisory Committee:
Professor John Ondov, Chair
Professor Doug English
Professor John A. Tossell

Dedication

Dedicated to my family,

Greg, Becky, and Kristin

Acknowledgements

I would like to thank those who pushed me to finish and those who made the last three years interesting and exciting:

To Ben, for your patience and support. For holding me up when I needed it most and giving me advice I rarely listened to, but probably should have taken.

To Greg, for everything. From the first lunch to the last drink. For the late night adventures, the numerous lyrical masterpieces and for your friendship.

To my roommates, Tayler, Sara, Katie, and Courtney, for your knowledge, support, and friendship.

To my friends, for the laughter and support you gave me.

To Dr. John Ondov for his dedication to his research.

Table of Contents

List of Tables

List of Figures

Chapter 1: Introduction

A. Overview

One of the fastest growing environmental and human heath problems facing the United States today is air pollution due to anthropogenic emissions sources. The United States Environmental Protection Agency (EPA) regulates the amount of particle emissions produced by industrial manufacturing and vehicular exhaust, as even low concentrations of fine particles emitted from these sources have proven to be detrimental to the environment. Pollutants which absorb radiation from the sun in the infrared wavelength range, such as CO_2, cause climate changes which are linked to the melting ice in the Artic and warming of the Atlantic Ocean (Seinfeld et al., 1988). Also, it has been shown that acid rain is caused by anthropogenic pollutants which in turn damages aquatic life and vegetation (Seinfeld et al., 1988). As a result, the need for stricter regulations on the largest polluters is more important now than in previous generations in order to significantly reduce the rate of environmental degradation.

Human health is also affected by the increase in fine and ultrafine particle emissions. From here in we will define ultrafine particles as particles with diameters less than 2.5 μm, or $PM_{2.5}$. $PM_{2.5}$ is known to be the most toxic to humans as they are made up of a mixture of soot, organic compounds, acid condensates, metals, and sulfate and nitrate particles (Dockery *et al*., 1993). Due to their size, fine particles can penetrate deep into the lungs, which can contribute to serious human health

problems including cancer, respiratory illnesses, or even death among the sick and elderly (Dockery *et al.*, 1993).

In 1997, the EPA reevaluated previous air quality standards and placed greater emphasis on ultrafine particle emissions (particles with diameter less than 2.5μm) during the establishment of the National Ambient Air Quality Standards (NAAQS). To monitor emissions, in-stack monitoring was implemented at some of the largest sources (power plants, municipal waste incinerators), but this method is time consuming and costly. To reduce the need for expensive in-stack measurements, stationary receptor sites have been used to collect highly time-resolved samples. Data from these samples can be entered into mathematical models to identify multiple pollution sources. There are two types of source apportionment models; receptor-based factor analysis and chemical mass balance models. The most widely used models include chemical mass balance (CMB) (Watson *et al.*, 1991), positive matrix factorization (PMF) (Paatero, 1997), UNMIX (Henry, 1997; Henry, 2000), and the pseudo-deterministic receptor model (PDRM) (Park *et al.*, 2005).

Factor analysis models generate factors which try to explain the variance in time series data based on which species are correlated, as these species are assumed to be from a common source. Ideally, the identification of source is possible because of tracers or combinations of elements that are unique to specific sources (Ondov *et al.*, 1998). For example, Se and As are known to be indicators for coal combustion (Gordon, 1988; Kidwell *et al.*, 2004), while Ni and V are tracers of oil combustion (Mroz, 1976; Olmez *et al.*, 1985), and Zn and Cd are marker species for municipal incinerators (Pancras *et al.*, 2005; Kidwell *et al.*, 2004; Greenberg *et al.*, 1978).

For the best results, receptor-based models should use as much information pertaining to actual physical conditions as possible, including meteorological data, elemental concentrations, and the locations of sources. The user must input the number of sources in the area when using factor analysis. From the model the source profiles are generated and interpreted by the user. The profiles are generic, but can be identified as specific sources after looking at wind directionality plots.

Conversely, chemical mass balance models require prior knowledge about the composition of particles from emissions sources to calculate the mass concentrations emitted from each source (Watson *et al.*, 1994; Gordon, 1988; Schauer *et al.*, 1996; Zhou *et al.*, 2004). Chemical mass balance models use generic source profiles which makes them less reliable as we known for example, different types of coal is used in different coal-fired power plants, which is comprised of different elemental species.

A receptor model utilizing both size and composition data inputs can increase the resolving power of the model because the age of the particles and proximity of the sources can be inferred from particle size (Whitby, 1978; Ondov *et al.,* 1998). In this project we used 4 particle size bins (< 80 nm, 80-300 nm, 0.3-1 μm, and 1-2.5 μm) and particle composition to apportion fine particle emission sources using positive matrix factorization.

B. Particle Size Distributions

The NAAQS reduced the allowable $PM_{2.5}$ mass concentration emitted by industrial and motor vehicle sources. However, pollution control strategies depend on the ambient aerosol data collection and the effectiveness of models used to

determine the particle sources. $PM_{2.5}$ is mostly from anthropogenic sources; however there is some contribution from vegetative burning and marine aerosols which is uncontrollable. Particles from combustion sources can be categorized into two groups; controlled or uncontrolled high temperature combustion. Uncontrolled combustion sources are mainly motor vehicles emitting diesel exhaust and sources which do not have pollution control devices such as electrostatic precipitators or scrubbers, to collect particles in the nanometer size range. Controlled high-temperature combustion emissions are from power generation plants, municipal incinerators, blast furnaces, cement kilns, paint manufacturers and more.

Research has shown that particle size distribution data can be used to improve the results found using source apportionment models (Park *et al*., 2004; Manoli *et al*., 2002). We know that particles emitted from distant sources are subject to dry and wet deposition, cloud and fog processing and atmospheric chemical reactions during transport, thus, by the time the transported particles reach a receptor site, they have increased in diameter size. For example, particles from regional sources increase in size largely by accumulating secondary mass from the oxidation of atmospheric gases (SO_2) (Ondov *et al*., 1998).

A previous study by Ondov and Wexler (1998) describes the particle size distribution paradigm (see Figure I below from Ondov *et al*., 1998) which was used to determine the ranges of the particle size bins in this study. From this and numerous other studies we know that nucleation particles (less than 80 nm) are emitted from uncontrolled combustion sources (eg. traffic) and are formed in the atmosphere by condensation of atmospheric gases, but the frequency of occurrence of these

nucleation events is still not well known. In any event, it is well documented that

nuclei particles account for little aerosol mass, in most cases. Condensation can

cause the formation of new particles, which is known as homogenous nucleation, or

deposit nucleation particles on existing atmospheric particles (Warneck, 1988). This

is known as heterogeneous condensation. Reactive gases, such as SO_2 or NO_x, often

correlate well with particles found in the less than 80 nm particle size range due to

condensation (Warneck, 1988). The atmospheric residence time of nucleation

particles is very short due to the rapid growth by coagulation and condensation.

Particles collected in the size range 80-300 nm are fresh aerosol particles

emitted from primary, local sources, such as controlled, high temperature combustion

sources (Ondov *et al*., 1998). Although, primary particles comprise of only a small

fraction of atmospheric aerosol mass; they are usually enriched by metals, which can

be used to identify sources (Ondov *et al*., 1998; Dodd *et al.,* 1991). Particles in the

fresh accumulation aerosol size range undergo cloud processing or atmospheric

reactions with other particles. For example, after SO_2 is emitted from a power plant,

it is oxidized by cloud droplets and converted to H_2SO_4 during transport (Ondov *et

al*., 1998). On particularly humid days and/or periods of stagnation particles emitted

in this size range undergo condensation by water vapor, which causes particle growth

proportional to relative humidity (Ondov *et al*., 1998). Fresh particles that have been

transported by wind movement from regional sources will be found in the transported

aerosol size range.

Particles found in the size range from 0.3-1 μm have spent more time in the

atmosphere than the fresh accumulation particles of the 80-300 nm range – such that

they have accumulated more secondary aerosol mass. These particles have undergone atmospheric growth processes during transport. It is common to resolve secondary sulfate in this size bin as much of the sulfate is transported from the Ohio River Valley power plants at distances of up to 800 km. This "aging process" is accelerated by cloud processing that is facilitated as air crosses the Appalachian Mountains as mentioned above. Particles from local sources that are emitted during periods of stagnation can also grow by condensation before reaching the detection site. Secondary sulfate has a long atmospheric residence time, which is why we can see the large mass contribution of sulfate particles from the Ohio Valley power plants.

Coarse particles (1-2.5 μm) are from local road dust or occasionally from distant sources if the particles have been aloft for a few days, known as "aged aerosol" (Warneck, 1988). Larger, coarse particles have a short residence time if they are from mechanical processes including road dust, pollen, and other types of dust from soil or motor vehicle breaks. The four particle size bins mentioned are illustrated in Figure I by Ondov and Wexler (1998).

Figure I Aerosol paradigm from Ondov and Wexler, 1988. Four particle size bins mentioned are shown undergoing aging and particle growth by condensation or hygroscopic growth. Nucleation particles are from uncontrolled combustion sources in the > 80 nm size range. Fresh particles in the accumulation aerosol range undergo hygroscopic growth as they are released from the smoke stack, but this process is reversible and depends on the RH. SO_2 will undergo irreversible conversion to H_2SO_4 which has a long atmospheric residence time. Transported particles are found in the aged particle range. Aged and coarse particles have a short residence time due to increased settling velocity.
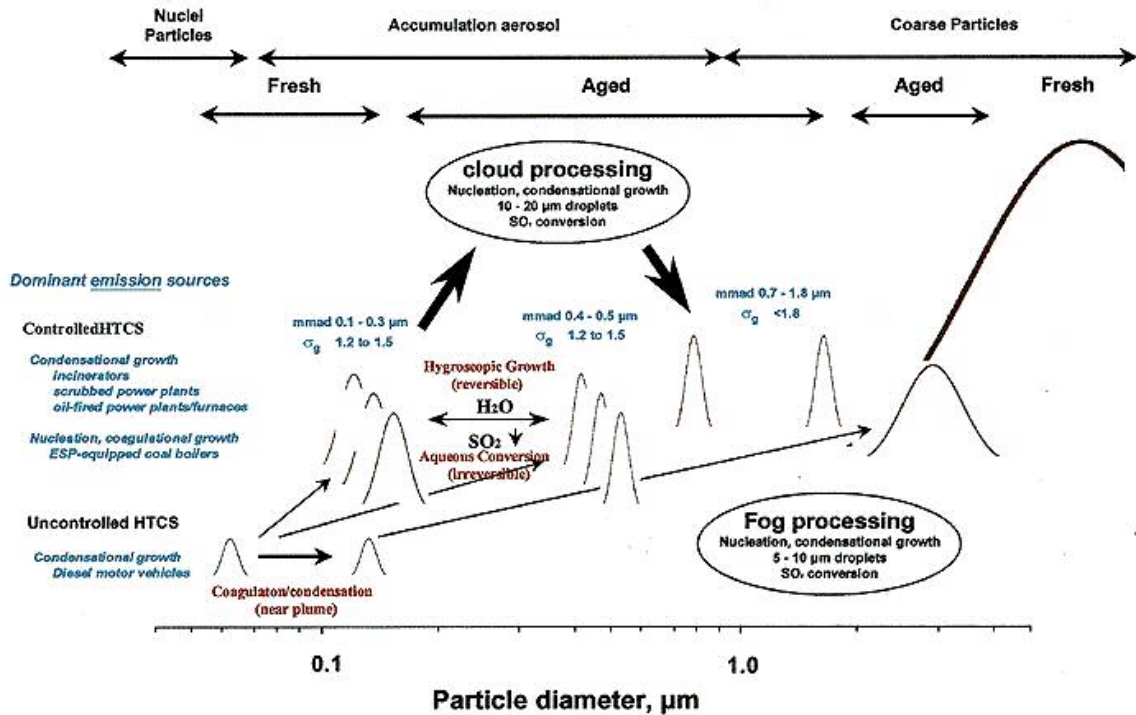
C. Site Description

Baltimore is the largest city in Maryland (population 650,000) with the one of the busiest ports in the United States. The city is located at the head of the Patapsco River about 40 miles north of Washington DC. It is southwest of Philadelphia/New York City corridor making it an epicenter for Northeast air pollution from commuter traffic. Also, located 150km to the west lay the Appalachian Mountains and the Ohio River Valley, a power plant 'hot spot'. The sampling trailer was located on Ponca Street in Baltimore, MD (39.2891º, -76.5546º). It is 1 km from the I895/I95, a major interstate merging point. Directly across the street from the site is a bus maintenance facility and there are 3 toll facilities (Fort McHenry tunnel, Harbor Tunnel, and the

Key Bridge) in the vicinity, that approximately 30,000 diesel trucks use each day. There are multiple major traffic arteries, including I95 running from Boston, MA to Miami, FL, I895, and the Baltimore Beltway, I695, which creates a complex system of particle line sources. There are two waste incinerators less than 15 km from the site and Constellation Energy owns and operates 4 coal and oil-fired power plants in the Baltimore region and numerous others lying just outside the metropolitan area, adding to the total fine particle emissions mass. See Figure II for a further description of emissions source locations.

Figure II Metal PM$_{2.5}$ emissions sources in the Baltimore region
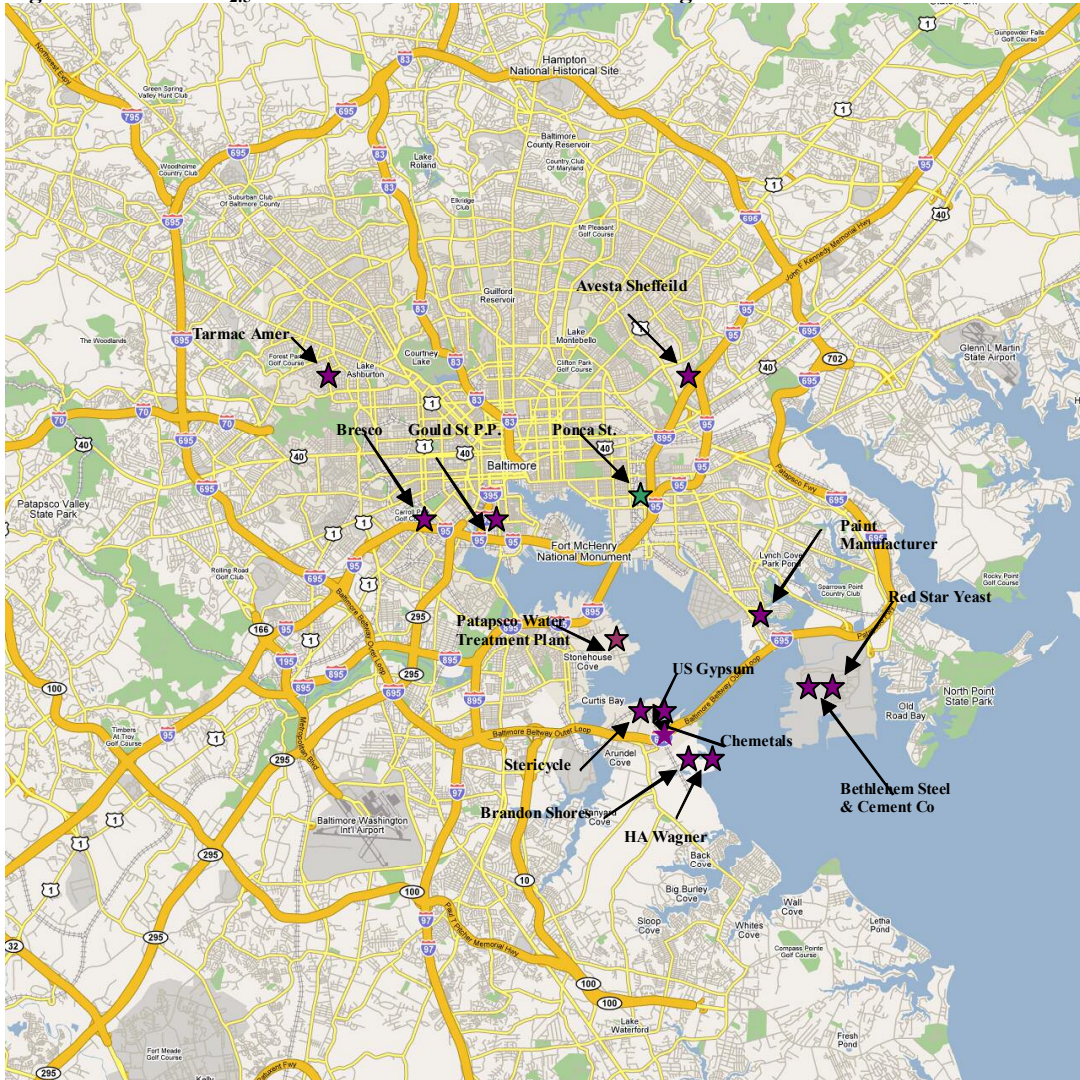
Chapter 2: Experimental

A. Data Sets Employed

The objective of this research project was to use discrete particle size bins which give information about source type, age of the particles, and transported distance of the particles for source apportionment. We separated the project into three studies: a time series analysis and two positive matrix factorization models. In our first PMF analysis, we used the model to assign metal particles, as well as gases, EC/OC, sulfate, nitrate, TEOM, and size distribution data, to emission sources in Baltimore area and the regional Northeast using data from July 20th to 22nd, 2002, herein referred to as Dataset A. We chose 6 sources based on results from principle components analysis (PCA) which showed that 6 factors explained 79% of the variance. A second data set was used, herein referred to as Dataset B, to investigate the effect of using a mass weighting to the size distribution data. This also has the desirable effect of eliminating some of the problems associated with mixed units and ambiguous uncertainties for number counts in the input matrix for the model. Dataset B only covered July 21st and 22nd because there were missing data points on July 20th. Values were extrapolated to fill in the missing values in Dataset A, but we felt our results would be more reliable if we omitted these data points altogether, so we only included measurements from the 21st and 22nd in Dataset B. Dataset B contained particle mass concentration size bins instead of particle count size bins. When number counts were used, the bin containing the smallest particles (< 80 nm), has very low uncertainties because there is an enormous amount of particle counts eg. at 6:30 on July 21st there are > 500,000 particles counted in the < 80 nm size bin

while only 86,000 in the 80-300 nm size bin and 85 in the 1-2.5 μm size bin. Thus, the relative standard deviation calculated by the square root of the count is substantially smaller for the < 80nm bin than the 1-2.5 μm bin. PMF uses the uncertainties to weight the data; therefore the < 80 nm size bin is weighted as having more contribution associated with each factor creating an unrealistic source profile for say, a dust source.

The addition of particle mass concentration to the model eliminated the meaningless dimensionality of the PMF results when the input data matrix had mixed units of number counts and concentrations. PMF calculates the source profiles as the magnitude of the species measured relative to the sum of all species. Thus for the modeled Dataset A, the profile had units of approximately mass/m^3/no. of particles/m^3 of air. The units for the source profile for Dataset B was represented as mass of species/m^3/sums of mass/m^3 of air. Thus, dimensionality of the results was restored when we created our second data set (Dataset B) using particle mass concentrations. Gas and TEOM (total PM$_{2.5}$ mass concentration) data was eliminated from Dataset B. TEOM data was omitted because the particle size bins already contained the PM$_{2.5}$ mass concentration in the particle size data, thus using TEOM data in the model would have been redundant. Gas data was eliminated because we were using mass concentration units. A summary of the input data for the model is shown in Table I.

Table I. Instruments and measurements made at the Ponca Street Supersite. (Note – all data was averaged/interpolated to thirty minutes for the PMF data matrix)

Instrument models	R&P 8400N	Harvard	TSI APS/SMPS	SEAS	Federal Reference Monitors	R&P TEOM	Sunset Labs
Species measured	Nitrate	Sulfate	Size bins: 0.487-20.5 µm	Al, As, Cd, Cu, Fe, Mn, Ni, Pb, Se, Zn	NO, NO_2, NO_x, O_3, CO	PM2.5 mass conc.	EC/OC
Time series	10 min.	20 min.	5 min.	30 min.	10 min.	30 min.	1 hr
Reference	*Harrison et al, 2004; Weber et al., 2004; Stolzenburg et al., 2000*	*Harrison et al., 2003; Ondov et al., 2004*	*Park et al., 2006*	*Kidwell et al,. 2001*	*Park et al., 2006*	*Park et al., 2006; Lee et al. 2005*	*Park et al., 2004*

Each instruments used to collect the sample datasets have been described elsewhere (see Table I for references). The Semicontinuous-Elements in Aerosol Sampler-II (SEAS-II) is an aerosol particle concentrator designed to collect particles as small as 80 nm in thirty minute intervals. The instrument is built solely of glass and plastic components to eliminate any metal contamination. The particles are grown by steam injection with repeated cooling until they have grown to a size of >3 µm. The grown particles are concentrated through a virtual impactor and collected by an automated fraction collector. Each slurry sample is placed in a clean, labeled vial and stored in a freezer until analysis. A detailed description of the SEAS can be found in Kidwell and *et al.,* 2001 and 2004; and Pancras *et al.,* 2004.

The slurry samples were analyzed for 11 metals (Al, As, Cd, Cu, Cr, Fe, Mn, Ni, Pb, Se, Zn) using the Perkin Elmer simultaneous multi-element electrothermal atomic absorption spectrometer (SIMAA 6000) with Zeeman background correction.

The elements were analyzed in three analytical groups based on their furnace firing conditions and spectral interferences. The procedure for SEAS metal analysis by the GFAAS is detailed elsewhere (Pancras *et al*., 2004).

Size distribution measurements were made every five minutes at the site using a scanning mobility particle sizer (SMPS, TSI model 3080) and an aerodynamic particle sizer (APS, TSI model 3321). The SMPS collected particles with aerodynamic diameters between the sizes of 0.009-0.437 μm and the APS covered the range of 0.486-20.535 μm. There were more than 100 size bins total. Particles in these bins were summed and distributed into four sized bins representative of the nucleation mode, fresh combustion, transported and/or secondary aerosol, and coarse particles (50-80 nm, 80-300 nm, 0.3-1 μm, and 1-2.5 μm respectively) as mentioned earlier.

Total $PM_{2.5}$ mass concentrations were measured with a tapered element oscillating microbalance (TEOM).   The mass of the particles is measured by the frequency change of an oscillating tube. As the particles are deposited on a filter the oscillations decrease. The rate of flow through the filter is used to calculate the mass concentration of particles as a function of time. TEOM data was not included in dataset B, however, it was used to verify that the calculated particle mass concentrations from the size distribution number counts agreed with the particle mass concentrations measured (see Figure III).

B. Calculating Particle Masses for Data Set B

To calculate the mass concentrations of particles in the four size bins, the densities of particles in each of the 52 size bins were estimated from previous studies by Seinfeld *et al*. (1998) and Hinds (1999). The densities used for calculations of particle masses are shown in Table II. When the relative humidity was considered high, exceeding 85%, densities for particles with diameters falling between 0.6 μm and 2.5 μm were decreased to 1.2g/cc to compensate for water vapor condensed on these particles. Particle densities in the two smallest size bins remained the same during periods of high relative humidity as we consider these particles to be from either uncontrolled and/or fresh combustion sources and therefore are assumed to have not undergone homogenous condensation.

Table II. Particle densities implemented for the calculations of particle mass distributions

Particle Diameter Range (nm)	9.65-47	50.5-583	626-965	1037-2458
Densities (g/cc) low RH	2.5	2	2.5	2.2
Densities (g/cc) high RH	2.5	2	1.2	1.2

The masses were calculated for the 52 size bins and totaled to get a $PM_{2.5}$ mass concentration. This value was compared to the measured TEOM (total $PM_{2.5}$ mass) mass data which gave a R^2 of 0.75. The correlation between the measured and calculated particle masses is shown in Figure III.

Figure III. Calculated particle mass from SMPS/APS vs measured mass from TEOM
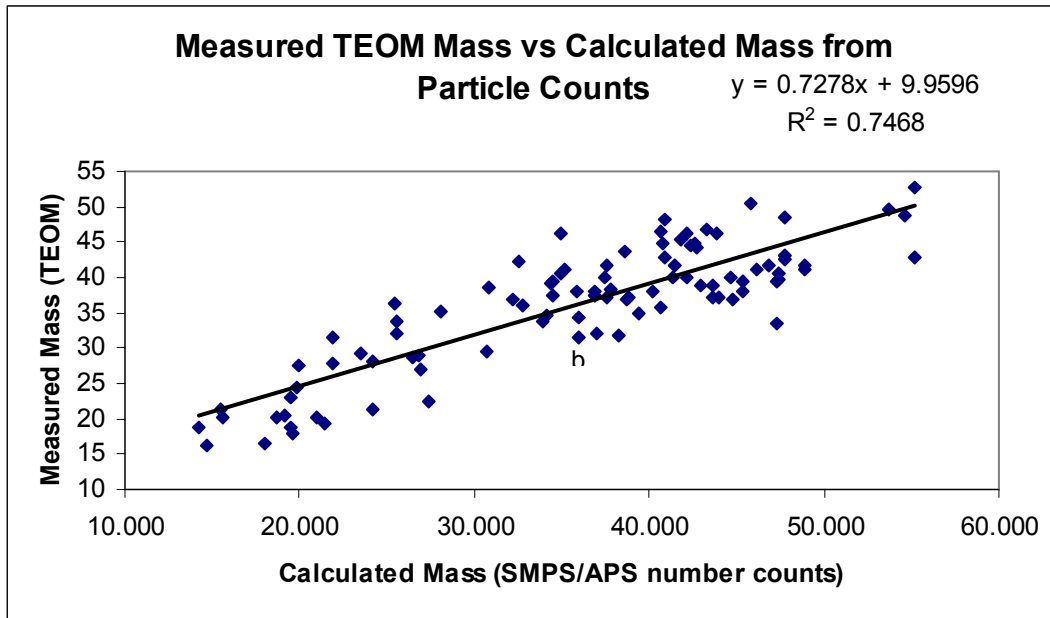
C. Nitrate and Sulfate Corrections

Data corrections were made to the sulfate and nitrate concentration data based on the assumption that all atmospheric sulfate and nitrate particles are neutralized by ammonium. The monitors measure the sulfate and nitrate concentrations without accounting for the mass of ammonium. To calculate the actual concentration of sulfate and nitrate, the measured values were multiplied by their mass fractions, a factor of 1.37 and 1.29, respectively. That is, the ratio of the molecular mass of ammonium sulfate (132.144g/mol) to sulfate (96.06g/mol) is 1.37 and the ratio of ammonium nitrate (80.04g/mol) to nitrate (62g/mol) is 1.29. These corrected values were used in Dataset B.

D. Positive Matrix Factorization

     Positive matrix factorization is a mathematical technique used to create two matrices representing source contributions and source profiles using a weighted least squares approach. PMF seeks to create a matrix with a minimum set of new variables using linear combinations of the old variables. The factor analysis model in elemental form is shown in Equation 1. Factors g and f are the source contributions as a function of time and the factor loadings, respectively (Paatero, 1994).

$$X_{i,j} = \sum_{k-1}^{p} g_{i,k} f_{k,j} + e_{i,j} \qquad \text{Equation 1}$$

$X_{i,j}$ is the jth species concentration measured in the ith sample, while $g_{i,k}$ is the mass contribution from the kth source contribution from the ith sample, and $f_{k,j}$ is the kth source contribution from the jth species. The variable $e_{i,j}$ contains the matrix of residuals used for the fit of the model.

$$e_{i,j} = x_{i,j} - \sum g_{i,k} f_{k,j} \qquad \text{Equation 2}$$

     PMF calculates a solution to an object function, Q (Equation 3) by least squares minimization. The standard deviations of the measured data ($s_{i,j}$), where s is used to weight the data. The g and f factors are solved simultaneously as the Q function is minimized. Q is the chi-square of the model. The calculated Q value should be approximately the same value as the number of data points in the input matrix for the most reasonable results (Hopke *et al*., 1999; Song *et al*., 2001).

$$Q = Q(G,F) = \Sigma \; \Sigma (e_{i,j}/s_{i,j})^2 \qquad \text{Equation 3}$$

PMF results are constrained to be non-negative, thus eliminating unrealistic source profiles. That is, there are no negative source contributions ($g_{j,k} \geq 0$) and there are no negative species concentrations ($f_{k,j} \geq 0$).

Chapter 3: Results

A. Time series data

      To determine the time periods to use for analysis we plotted the wind direction data to determine a time when the prevailing wind direction favored plumes from power generators and industries located between 120° and 190° (see Figure I). From July 21st to the 22nd the wind swept across the port area from the northeast to the southwest as can be see in Figure IV where the wind angles range from 30° to 200°. The mean wind speed was 3.7m/s with the fastest wind speed reaching 7m/s. Large variations in wind direction over short periods time make the use of highly time resolved data especially important, so that sources do not get over looked due to data averaging. The wind direction and wind speed for July 21st and 22nd are shown in Figure IV.

Figure IV. Time series plot of Wind direction and Wind speed

Wind Angle and Wind Speed
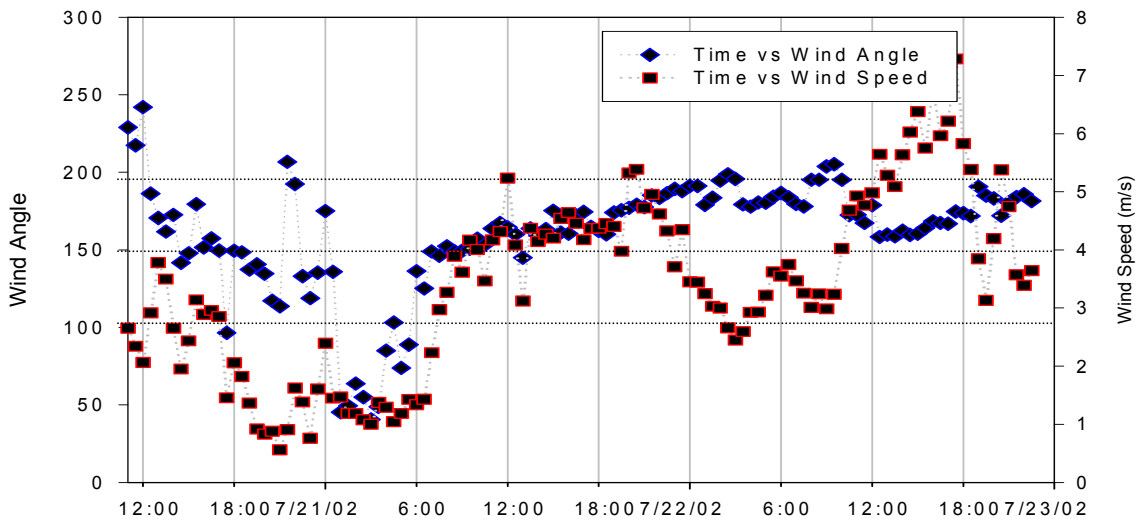
SEAS metals, gases, elemental and organic carbon, sulfate and nitrate concentration time series data are plotted in Figure V. Before utilizing the factorization model it is important to identify possible sources from peak concentrations and wind direction. To decide how many factors would be calculated in the PMF model we found times when concentrations of marker species reached a peak maximum and then tried to identify a source by wind direction at the given time of the peak. We identified five sources from our time series analysis described below. We expected that the model would find at least one more source that could not be seen without a mathematical model.

The most obvious source to look for is the coal fired power plant, Brandon Shores, located at 170° from the site. Selenium peaks six times during our study period (on July 21st at 11:30, 13:30, and 21:00 and on July 22nd at 8:00, 12:30, and 18:00). Each Se peak occurs when the wind angle is between 170º and 180°. From Park *et al.* (2005) we know that the ratio of Zn:Se concentrations should be ~1.8 in coal-fired power plant plumes. From 12:30 – 22:30 on July 21st the ratio of Zn:Se is 1.2, which is also the time when the wind speed is steady, averaging 4 m/s, and the wind angle aligned with the station angle of Brandon Shores (160° to 180°). We also see that sulfate peaks correlate well with the Se peaks, which is another indication that this is a CFPP. We also see nickel peaks at 16:30 and 18:00 on July 22nd when the wind is coming from 170º, which is the direction of an oil/gas-fired power plant, H.A. Wagner. Based on the assumption that we do not see NO, NO_2, or Ni peaks on the 21st when we see Se peaks from Brandon Shores, we think that the H.A. Wagner was shut down on the 21st and turned back on the 22nd. This is a reasonable

19

assumption because oil fired power plants are more expensive to run, therefore they are only used when the extra energy is required.

The third source we identified was thought to be an incinerator. We saw a spike in Cd concentration at 19:30 on July 22nd when the wind is coming in from 190º. Cd is a tracer for burning plastics and often indicates municipal or medical waste incinerator source. There is a municipal incinerator located at 250º, BRESCO, and there is medical waste incinerator located at 190º, Stericycle. During the 2+ day study period the wind is does not come from 250º, therefore we attribute the Cd peak to Stericycle. Shrock *et a.l* (2002) measured the ratio of elemental species to Zn in an in-stack monitoring study at a medical waste incinerator in Miami, FL. They found the ratio of Cd:Zn was 20.1±22.3, which agrees with our results when the wind angle is aligned with the station angle of Stericycle at 190° between 19:00 and 20:30 on July 22nd. We found the ratio of Cd/Zn at this time to be 21.5. Table III is a comparison of our results with the in-stack measurements at the medical incinerator in south Florida.

Table III. Comparison of the ratio of elements to Zn in a medical waste incinerator from in-stack sampling and our time series SEAS metals concentrations from the Ponca St. site (mg of element: g Zn)

|	Medical Waste Incinerator-Miami, FL (1995)	Stericycle-Baltimore, MD (2002) Time series analysis
Cd	20.1±22.3	21.5
Cu	45.4±6.7	94
Fe	81.0±11.6	2000
Pb	159±24	139

We attribute the high ratio of Fe:Zn, and to some extent Cu:Zn, to be from the differences in measurement techniques used in the two studies and the high total concentration of Fe measured during our study period at the site. We measured concentrations at a receptor site, a location where there were very high concentrations of Fe numerous times from multiple sources, while the study done in FL was an in-stack monitoring analysis. The measurements taken inside the stack were only influenced by the incinerator emissions. Our tracers for medical waste incineration ratio's, Cd:Zn and Pb:Zn agree within 10%, therefore we expected to see an incinerator factor in our model results.

We believe that there is a traffic plume on July 21st at 3:00 when the wind direction is coming from 40º. At this time we see a peak in Fe concentration which is a marker for motor vehicles, but there are many other sources, including numerous other roadways located very close to the site, which contribute to the total Fe concentration. Because there are so many concentrated motor vehicle locations around the site, it is difficult to identify traffic emissions using only the time series data. For example, Route 895 turns northeast, heading away from the Ponca Street site which creates a line source for motor vehicles at 30º, but I95 runs south at 180º before making a sharp turn, and I83 runs at 315° from the site. We expected to see a motor vehicle or roadway source including dust and uncontrolled combustion particles in our PMF results because the site is located close to multiple roadways.

We also see that sulfate is correlating with the ozone concentration. As expected, ozone peaks in the afternoon hours each day. This indicates that we should see a secondary sulfate event in the early afternoon hours. We expect to see particles

in the secondary aged aerosol size bin correlating with peaks in sulfate concentration during the daylight hours.

Figure V. Time series plots from July 20th 11:00 to July 22nd 23:00 of SEAS metals, gases, EC/OC, sulfate and nitrate concentrations
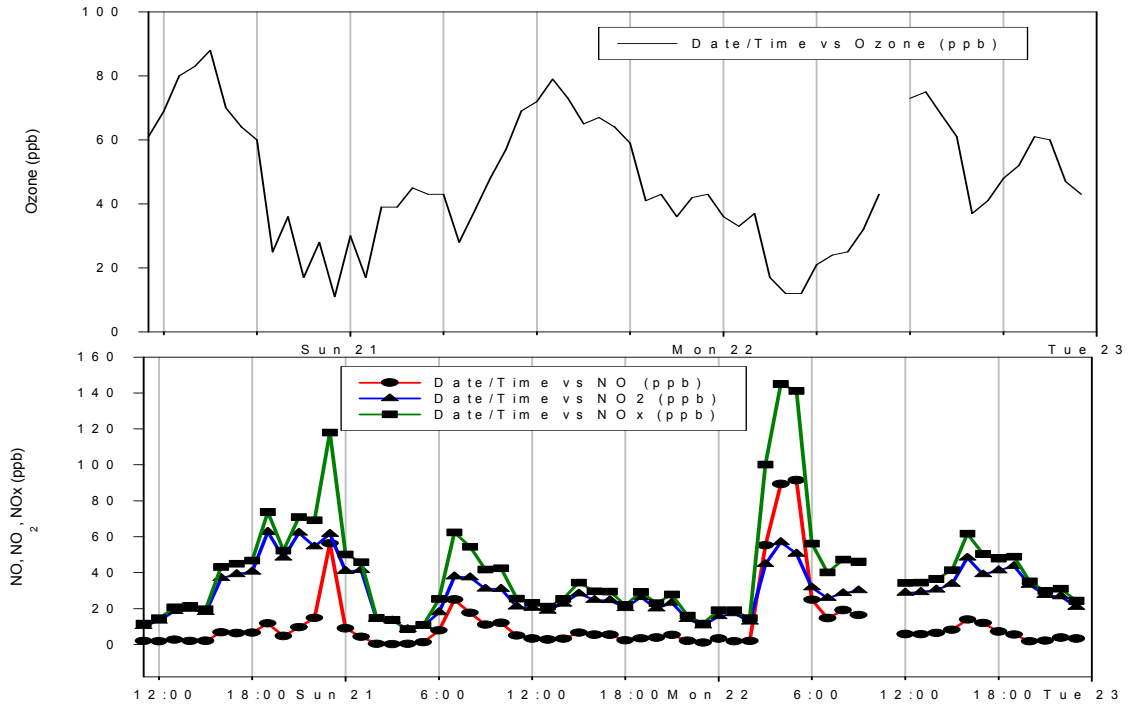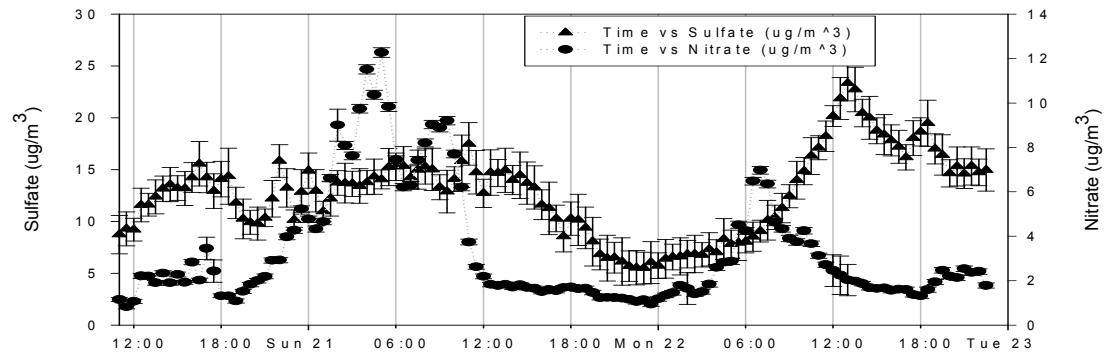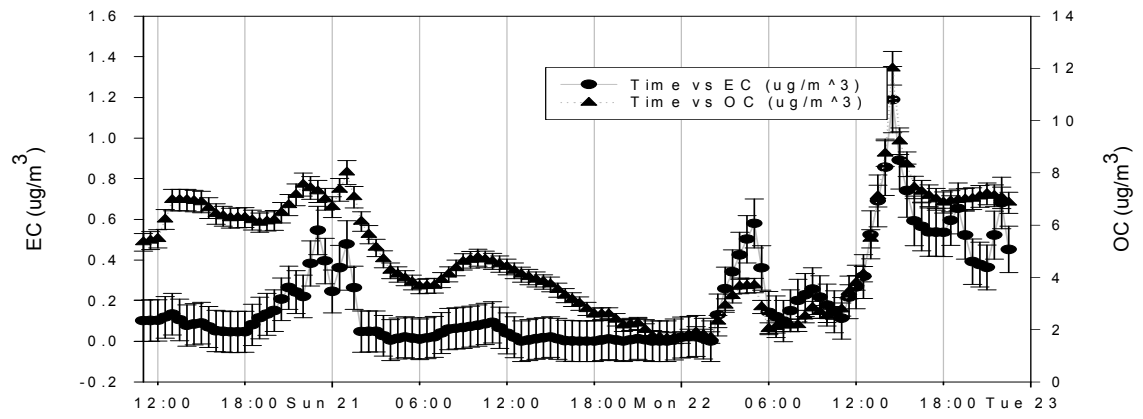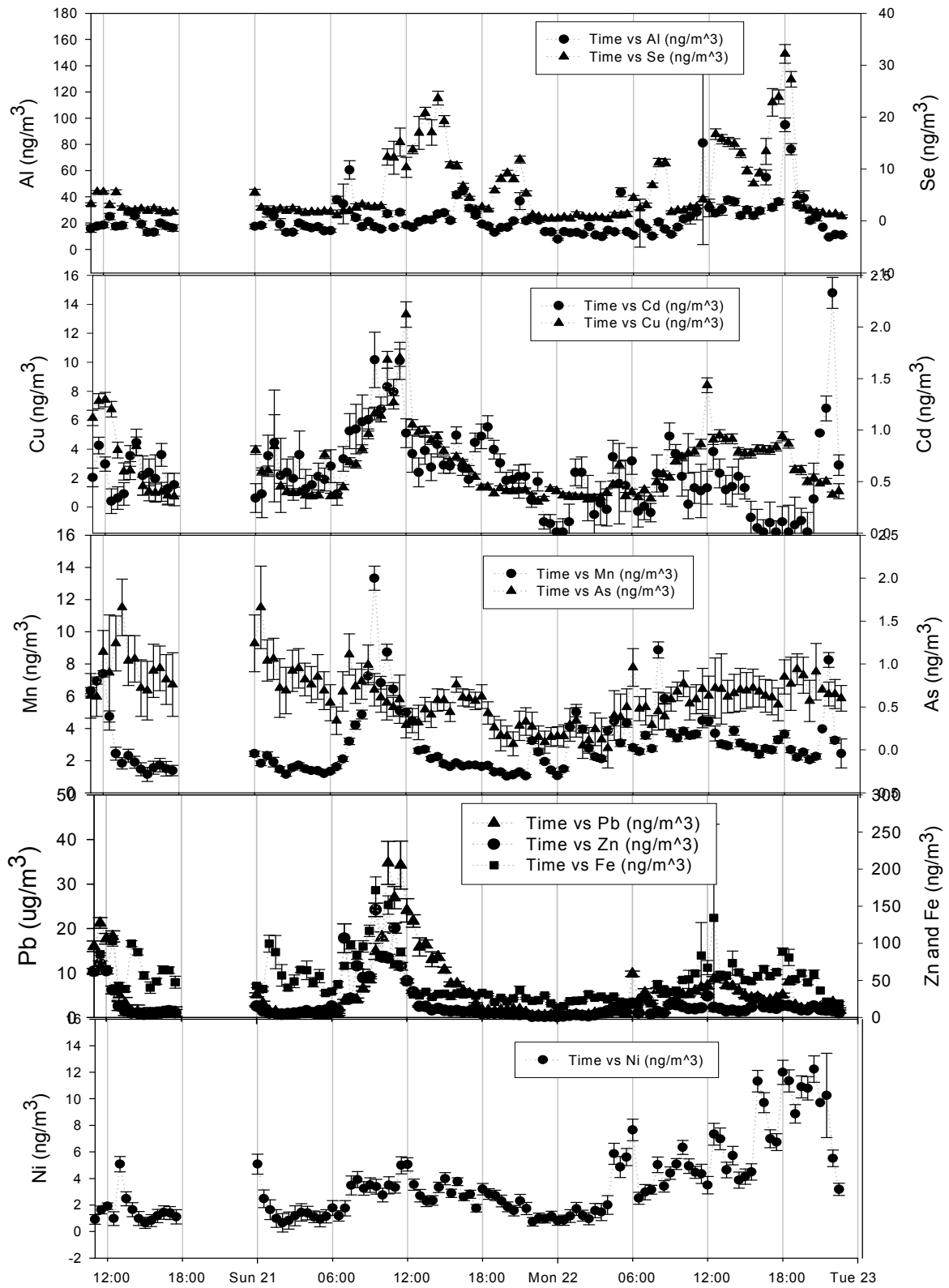
B. Comparison of PMF results (Data Set A and Dataset B)

Elemental and size distribution data were summed or interpolated to 30 minutes from July 20 at 11:00 to July 22nd at 23:30 for Dataset A and from July 21st 00:00 to July 22nd at 23:30 for Dataset B. Dataset A (particle number count size bins) includes the gases and TEOM data while Dataset B (mass concentration size bins) does not. Table IV lists the sources identified by each dataset.

Table IV. Factors or sources found from Dataset A and Dataset B from PMF models

	Dataset A	Dataset B
Factor 1	Coal-fired power plant (Brandon Shores CFPP)	Coal-fired power plant (Brandon Shores CFPP)
Factor 2	Steel Plant (Bethlehem Steel)	Medical Waste Incinerator (Stericycle)
Factor 3	Diesel Emissions	Oil-fired power plant (H.A. Wagner)
Factor 4	Nitrate Event	Secondary Nitrate & Sulfate Partitioning
Factor 5	Secondary Sulfate	Secondary Sulfate and dust
Factor 6	Gas-fired power plant (H.A. Wagner)	

Our analysis of the PMF results is described below. There were three common sources between the two datasets, namely a coal-fired power plant, a secondary sulfate partitioning event, and a secondary nitrate event.

1. **Coal-fired power plant**

According the Maryland power plant research program, Brandon shore produces as much as 600,000 tons of fly ash per year.   We were able to identify the Brandon Shores power plant from PMF results using Dataset A and Dataset B. We see that from Dataset A, 59% of the Se is loaded on this factor (Figure VI(a)) and from Dataset B, 94% of the Se measured is loaded on this factor (Figure VII(b)). Kowalczyk *et al*. (1982) found that 90% of the Se measured in an urban area was from fresh coal combustion which agrees well with our results from Dataset B.

Typically, there are two size modes associated with coal fired power plant emissions; the fresh accumulation mode and a fly ash mode. The fresh accumulation particle size mode is a result of nuclei condensation inside the furnace and stack. Moreover, there are generally fresh nuclei particles formed by homogeneous nucleation in the plume after discharging into the atmosphere from the stack. The larger mode is from unburned fly ash not caught by the electrostatic precipitators or scrubbers (Ondov *et al.*, 1998; Markowski *et al.*, 1980). Figure VI(b), the factor score, and Figure VI(c), the source profile, show particles loaded into the fresh combustion bin, but it does not show the particles in the fly ash mode (0.5-1 μm). We do see the two particle size bins in Figure VII(d) where the particle size bins are represented by the area plot. From Figure VI(c) and Figure VII(c) we see that the source profile correlates with the time series data where we see five Se peaks during periods when the wind angle is approximately 170°.

There also seems to be a high concentration of sulfate from this factor, which can also be used as a tracer of coal-fired power plants. At the time the plume leaves

the CFPP stack, SO_2 undergoes an oxidation reaction (with OH·, O_2, and H_2O) to form H_2SO_4 in the atmosphere. Sulfate particles undergo homogenous oxidation in clouds or on wet aerosol particles causing an increase in particle size.

The wind direction when the Se and source factor are peaking is between 160° and 180º. This can also be shown in directionality plots (Figure VI(c) and Figure VII(e), which are plots of the wind direction vs the source profiles. This shows the exact location of Brandon Shores therefore we are confident that this factor from Dataset A and B has been correctly identified.

Figure VI. Coal-fired power plant source profile from Dataset A. Figure VI(a) shows that 59% of the Se is loaded on this factor while Figure VI(b) shows a high contribution from Se and sulfate. Figure VI(b) and Figure VI(d) show particles loaded in the fresh combustion bin and Figure VI(d) also shows a good correlation between the Se time series data and the G factor loading from the PMF results. Figure VI(c) shows the directionality plot which tells us the source is at 170º.
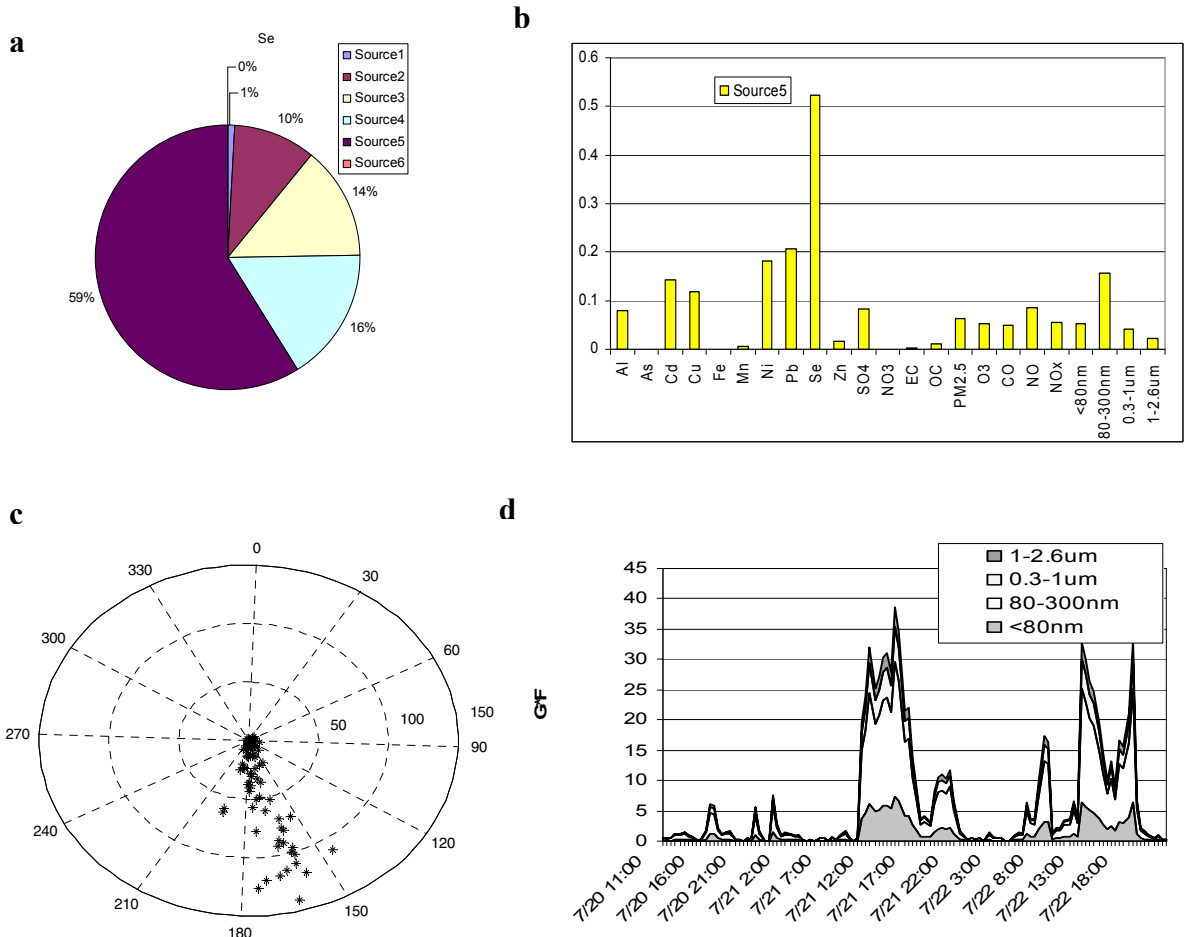
Figure VII. Source profile for a coal-fired power from Dataset B. Figure c shows the correlation between the G factor score and the concentration of Se in ng/m³ vs time of day. The size distribution graph shown in figure a is an area plot which shows that most of the particles emitted from this source are in the 80-300nm size range, supporting our hypothesis that this factor is from a fresh combustion source. Figure b is the distribution of Se between the 5 sources; showing that 94% of the Se is loaded on to this factor, which is a good indication that this is a coal-fired power plant. The source profile shown in figure d again shows a high contribution from Se on this factor. Figure e is the factor score vs wind direction

a

b

Se Contribution to each source

c

Se and Source 5 Contribution

d

e

28
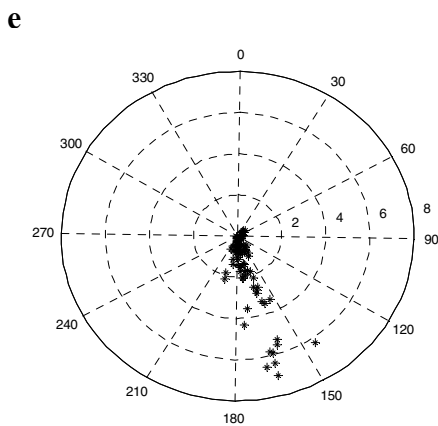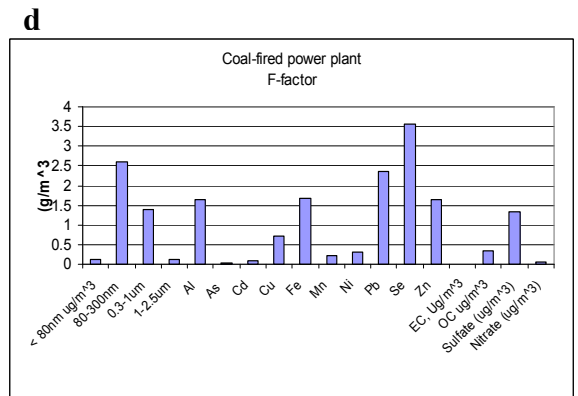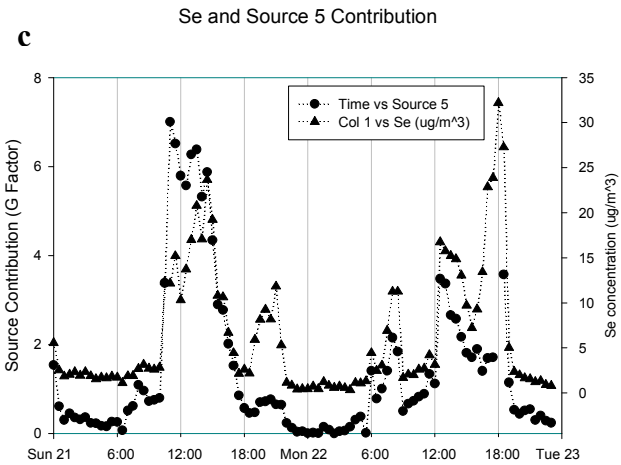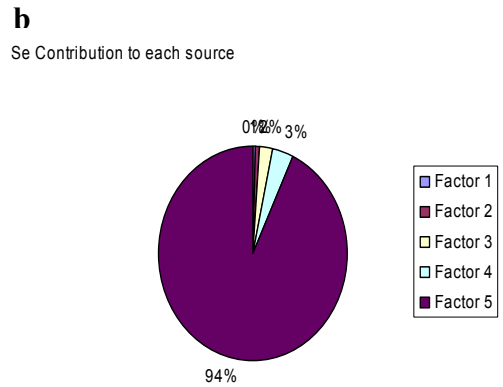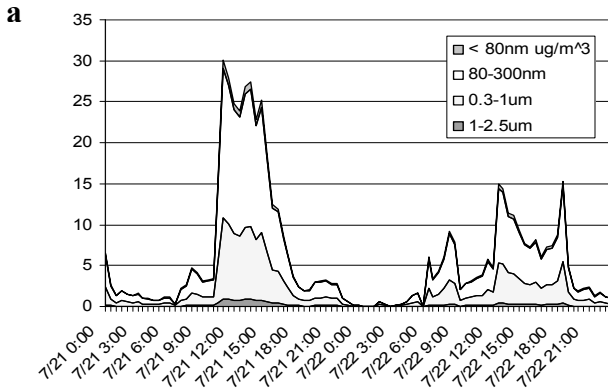
2. **Nitrate Event**

Factor 4 is believed to be a nitrate event based on the correlation of nitrate peaks with the source profile, the secondary, aged particle size mode, and the diurnal pattern seen in Figure VIII(c) and IX(d). Cooler, less humid temperatures are favorable for ammonium nitrate and HNO_3 formation. Nitrate forms from the reaction of NO_2 with OH at a rate of 10-50% per hour during the daylight hours when OH is abundant (Seinfeld *et al.*, 1998).

Gaseous HNO_3 is soluble in water indicating that we should see larger particles from condensational growth if this is, in fact, a nitrate event. The f factor (Figure VIII(b) and Figure IX(b)) shows a significant contribution from the aged or transported particle size bin. The particle size distribution graph (Figure VIII(c) and Figure IX(d)) also shows that the 0.3-1 μm particles are dominating. Also, from the area size distribution graph we see that the peak concentrations are occurring in the early morning hours on the 21st and the 22nd.

Relative nitrate concentrations are shown in the pie charts in Figure VIII(d) and Figure IX(a). Using number concentrations we found that 60% of the nitrate was loaded onto this factor and using mass concentrations we found that 85% of the nitrate was loaded onto this factor.

The directionality plots shown below (Figure VIII(a) and Figure IX(c)) show that there is not a point source contributing to this factor. Nitrate, unlike sulfate, is largely contributed to the atmosphere by motor vehicles, i.e. a dispersed source in the Baltimore area, and it can be seen in the wind plot that there is no directionality associated with this source. Traffic contributes to the total atmospheric nitrate

concentration which might be a contributing factor to the varying directionalities on

the wind direction plots.

Figure VIII. PMF results from Dataset A. Figure VIII(b) shows a large contribution from nitrate and transported and coarse particles on the F factor score. Figure VIII(a) shows that the nitrate is not coming from a unique source. Figure VIII(c) shows that the particles are loaded in the 0.3-1μm and 1-2.5μm size bins. Figure (d) shows that 60% of the nitrate is loaded on this factor.
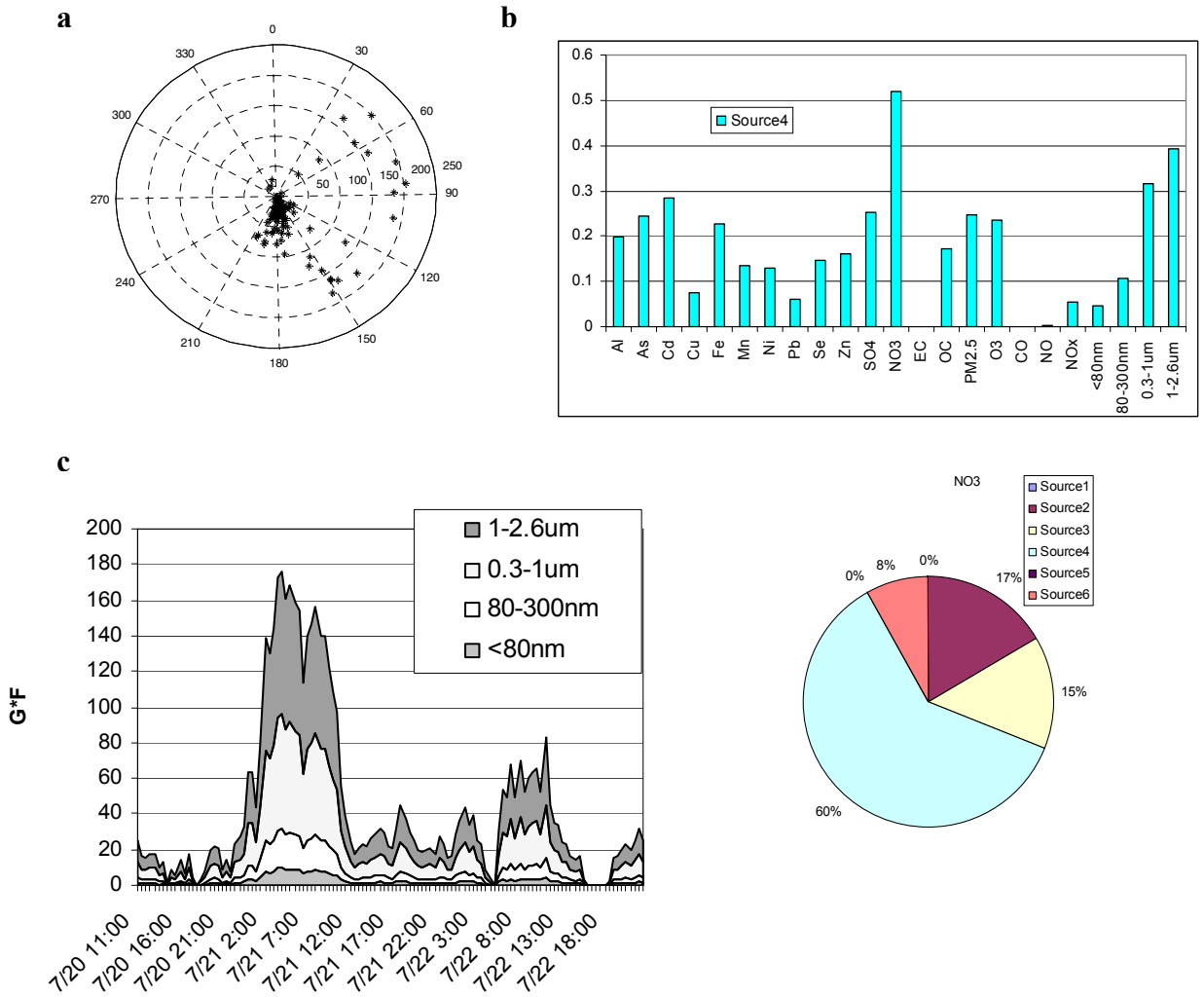
a

b

c

Figure IX. Nitrate Event from Dataset B. Figure IX(a) shows that 85% of the nitrate measured is loaded on this factor enforcing the idea that this factor has been correctly assigned as a nitrate event. Figure b shows the source profile, where again there is a significant amount of nitrate in the size range from 0.3-1μm as can be seen in figure d as well. The wind plot for this factor is shown in c.
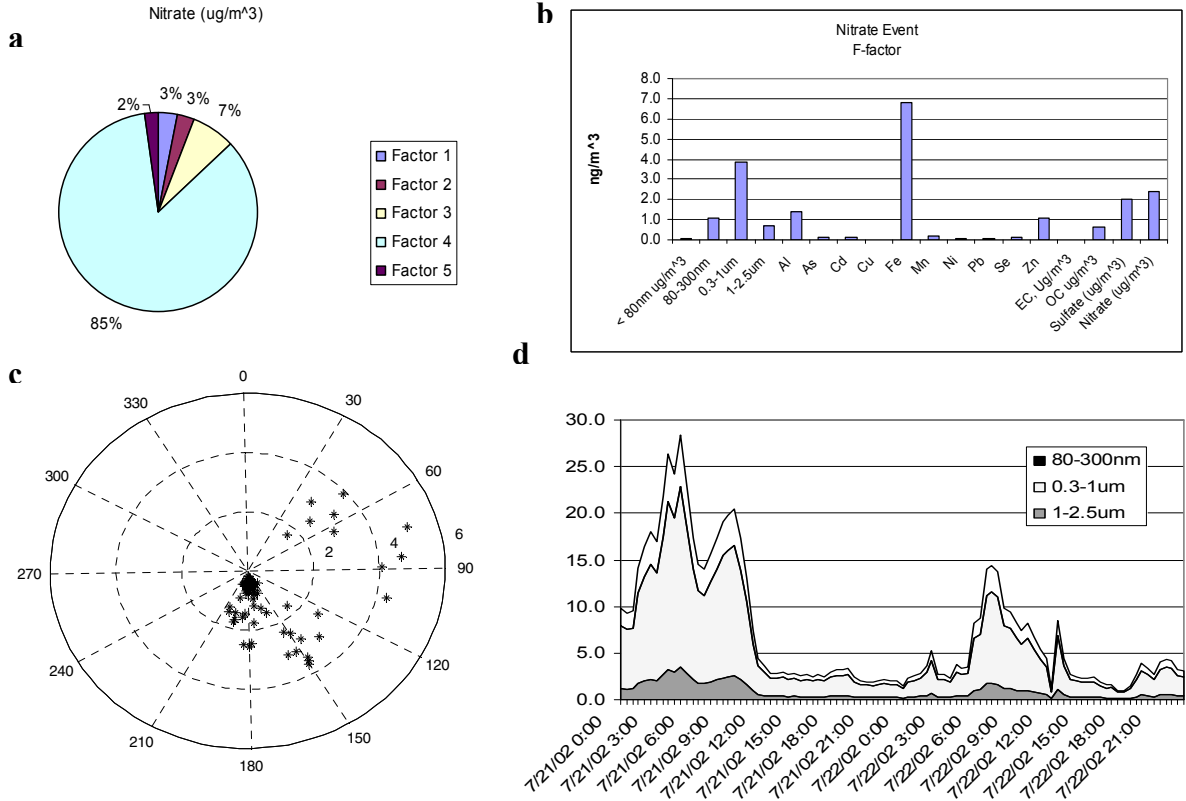
3. **Sulfate partitioning event**

We identified a third common factor as a secondary sulfate partitioning event. Sulfates in the atmosphere are classified as primary or secondary. Sulfur dioxide is the main pollutant from power plants; however, SO_2 has a fairly long residence time due to its slow reaction with OH·. Thus, secondary sulfate originates primarily due to the gas-to-particle conversion of SO_2 (Junge, 1954). Secondary sulfate particles tend to persist in the atmosphere and therefore can travel long distances from their source (Rodhe *et al*., 1981). The high humidity in the Northeast during the summer months

most often causes the sulfate to be found in the droplet mode, as shown from the results of the size distribution data and as reported by Ondov *et a*l. (1998). However, hygroscopic growth is reversible, so the aerosol size changes proportionally with relative humidity as it is transported.

The Ohio River Valley is one of the biggest contributors to secondary sulfates in the Baltimore area. Suarez *et al*. (2002) reported that 69% of the fine particle sulfate in Baltimore can be attributed to regional sulfate transported from sources upwind, more specifically, the Ohio River Valley where a large number of power plants are located. We found that 27% of the sulfate was loaded on the sulfate partitioning factor in the Dataset A analysis (Figure X(d)) and 34% of the sulfate is loaded on the factor associated with the sulfate event from Dataset B (Figure XI(c)).

 It can be seen in the size distribution plot in Figure X(b) that more than half the particles are loaded in the nucleation size bin while the other half are loaded in the fresh combustion size bin. On the other hand, Dataset B results show that most of the mass is loaded in the 0.3-1 μm size bin. Clearly this must be due to the difference in particle concentration weightings because the number counts are loaded in the small particle size bins when PMF weights the data by particle count, while the sulfate mass is loaded in the secondary aerosol size bin where particle mass is greater, but particle counts are lower when mass concentration weightings are used.

From the directionality plots we see the source contributing to this factor is from the SSE. This can be caused in part by Brandon Shores CFPP located at 180°. We can also see that the greatest peaks from the G factor scores occur around 12:00

each day. The high contribution from Fe in the f-factor score in Figure XI(b) is

attributed to iron sulfides from the power plant emissions.

Figure X. PMF results from Dataset A for the sulfate event. Figure X(a) is the factor loading for the sulfate event while Figure X(b) is the G factor score and particle size distribution graph. Figure X(c) is the directionality plot showing most of the sulfate is from the SSE. There is 27% of the sulfate loaded on this factor as shown in Figure X(d) and Figure X(e) shows the Sulfate concentration correlates with the G factor (b).
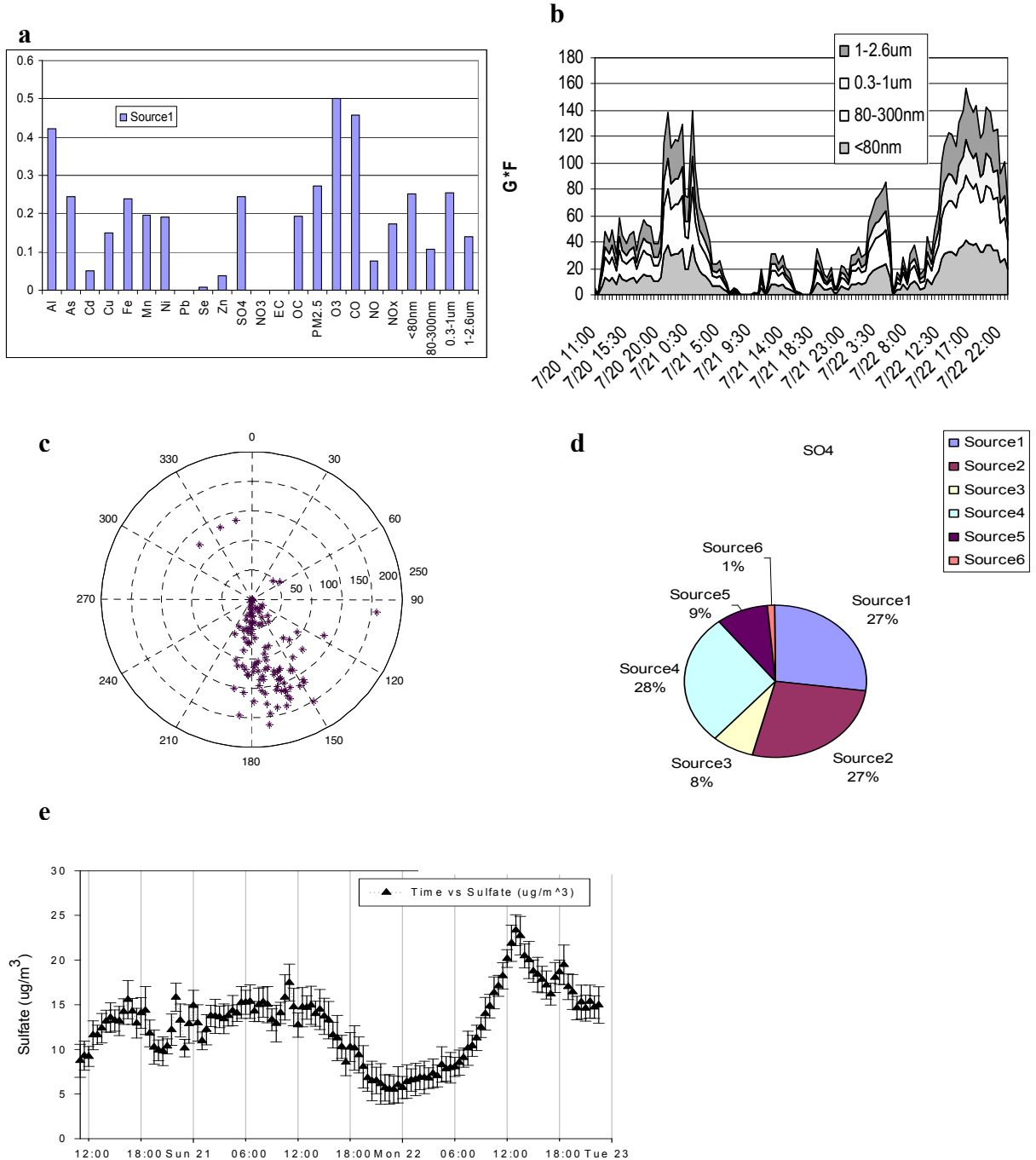
Figure XI. Sulfate event source profile from Dataset B. This factor shows a contribution from the large growth particles (0.3-1µm) from the area plot seen in Figure XI(a). The factor loadings in Figure XI(b) shows a contribution from sulfate, and the plot shown in Figure XI(c) shows that sulfate is contributing 34% to this factor. The directionality plot is shown in Figure XI(d).

a

b

c

Sulfate (ug/m^3)

d
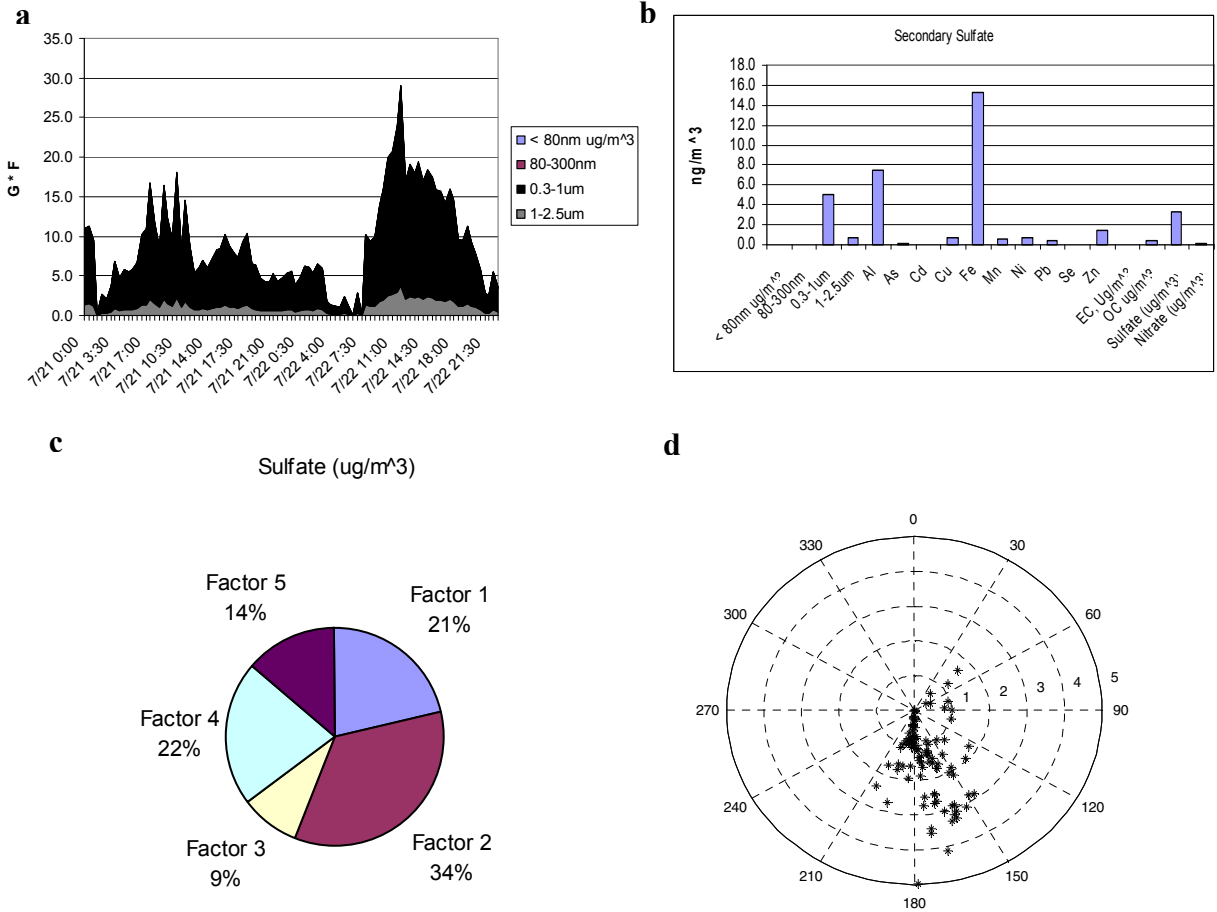
4. **Medical waste incinerator factor**

There is an incinerator, Stericycle, located at 190º from the site. Stericycle, Inc (5901 Chemical Rd, Baltimore) is the largest medical incinerator in the United States, handling over 600 million pounds of waste annually. It provides services to 48 states, the District of Columbia, five Canadian Providences and Puerto Rico.

As shown in Figure XII(d), there is a high concentration of Zn, Cd, Cu, and Pb, which are tracers of metal emissions from incinerators (Law *et al*., 1979).

34

Between 19:30 and 22:00 on July 22nd we see a large peak in the source profile for this factor (Figure XII(b)). This time period correlates with the time we believed to see a medical waste incinerator during our time series data analysis. The Cd/Zn, Pb/Zn agreed with Law *et al*.'s (1979) results.

Also, a study by Kowalczyk *et al*. (1982) in Washington D.C. showed that Cd from a refuse source is 35.5% of the total ambient Cd concentration using a chemical mass balance model. From their model results they found that the Cd concentration associated with a refuse incinerator was 0.64ng/m^3 while they predicted the total concentration of Cd to be 1.8ng/m^3, which agrees with the PMF factor results shown in Figure XI(a) where 35% is loaded on this factor.

The particles loaded on this factor are evenly distributed in the fresh combustion and transported aerosol size bins indicating the source is likely located in the Baltimore region, but there may be some absorbed H$_2$O vapor absorbed on the particles.

The wind direction is coming from 190º, the location of Stericycle, as shown in the wind direction plot in Figure XI(c). This correlates with our G factor peak occurring at 19:30 when the wind is blowing from 190º.

Figure XII. Incinerator source profile from Dataset B. Figure a depicts that 35% of the Cd measured is loaded on this factor. The area plot and the source profile in figures d and b respectively, show that particles on this factor are loaded on the 80-300nm size range. The wind direction plot shows the mass concentration associated with this factor is coming from 180°.

a

b

c

d
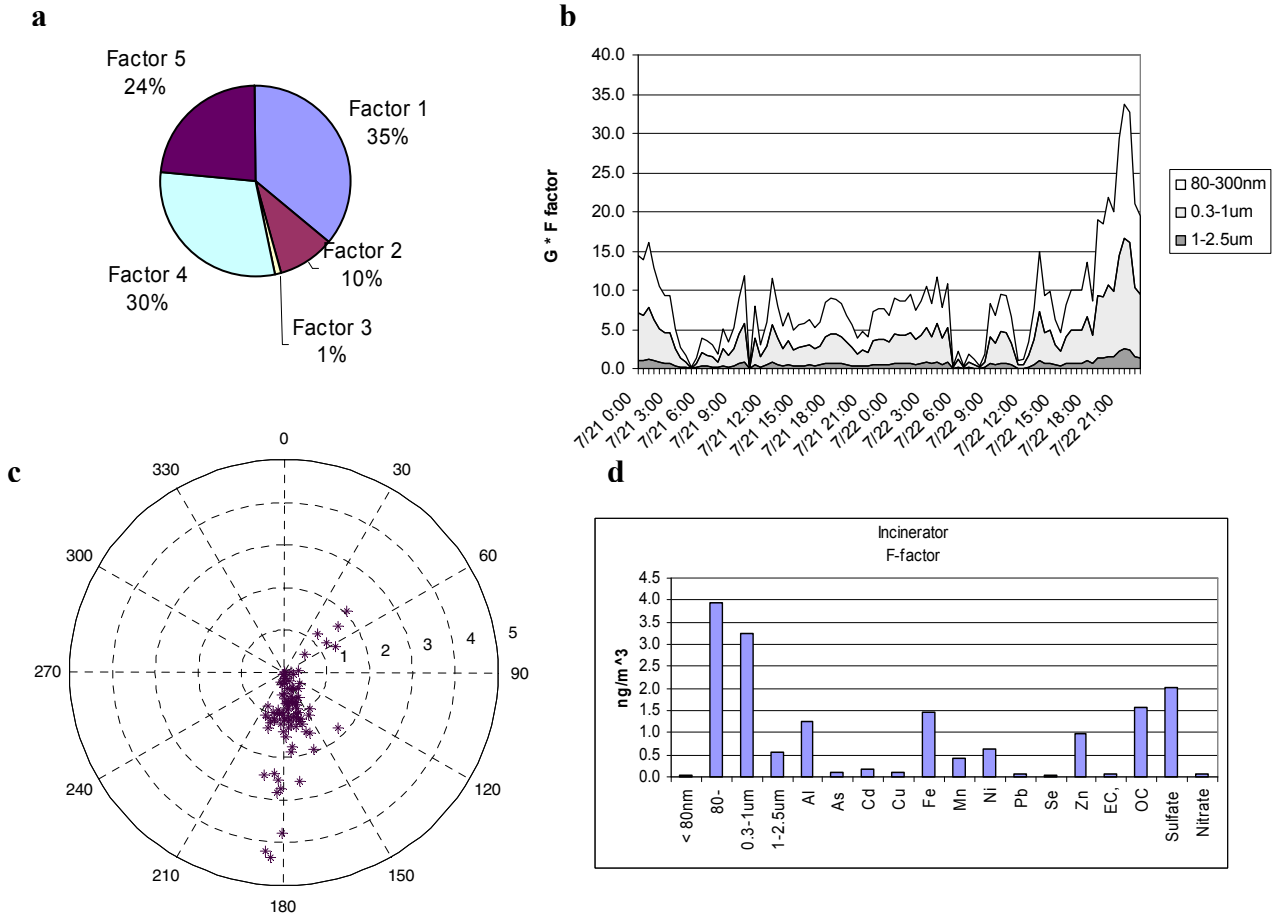
5. **Steel**

Maciejczyk (2000) studied the emissions from a steel plant and found that there are particle loadings on the fine particles as well as coarse particles as shown in Figure XII. Downwind from the Clifton site, the Fe particles were collected in the 1-10 μm size bin while the Se particles were collected in the 0.1-1 μm size bins. The

upwind plots show that the concentrations rose significantly when the steel plant emissions are blowing towards the site.

Figure XIII. Steel mill size distributions showing two distinct particle size bins for Fe
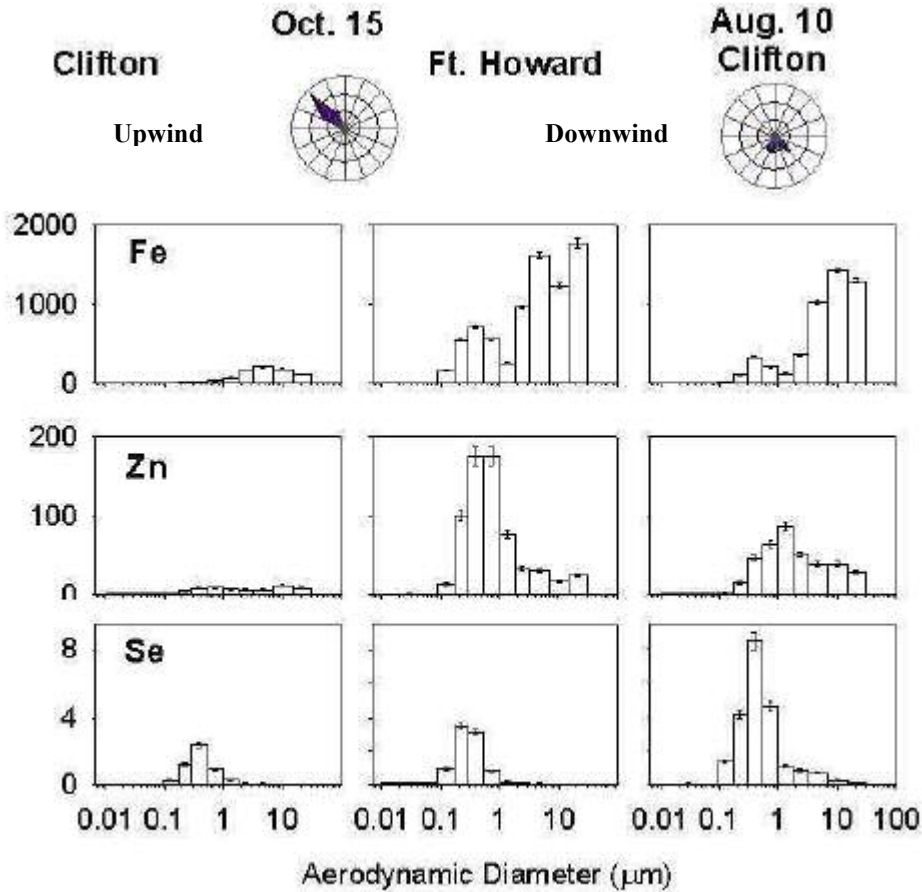
Baltimore is one of the largest producers of steel in the United States. There are two steel plants, Bethlehem Steel and Avesta-Sheffield blast furnace located in the Baltimore region. Bethlehem Steel is located less than 20 km at 144° from the site and Avesta-Sheffield blast furnace, also less than 20 km, and is located at a 75° angle from the site. The factor loading (Figure XIV(a)) shows a very high concentration of As contributing to this factor. As and Fe are well known marker species for steel production, which indicates this factor is likely from Avesta Sheffield or Bethlehem

37

Steel. Also, noting that Fe, Se, and Mn concentrations show peaks correlating only when the wind is blowing from 170º for this factor, implies there is only one steel plant contributing to this factor.   Figure XIV(b) shows the g factor where the plume arrives at the site approximately at the same time on the 20th and the 22nd (at 6am), but then we do not see the peak on the 22nd when the wind is coming from 180°.

We also find that 63% of Pb and 63% of Zn is loaded on this factor, which is shown in Figure XIV(d) and (e). This is not surprising because zinc and lead is found in steel manufacturing emissions.

Small (1979) found the ratio of As:Fe in a Bethlehem Steel plant plume to 0.0011. At 10:30 on July 21st we calculated the ratio of As:Fe to be 0.0036. This might be greater due to the increased wind speeds causing less dilution or improved instrumentation techniques.

The two particle size bins found by Maciejczyk (2000) are seen in the factor we identified as Bethlehem Steel (Figure XIV(a) and (b)) and we see a comparable As:Fe ratio to known measurements by Small, which means we were likely correct in our classification that this factor can be identified as Bethlehem Steel.

Figure XIV. Steel profile from Dataset A. Figure XIV(a) shows the source profiles-typical incinerator plumes show a high concentration of Zn and Pb. Figure XIV(b) shows the peaks occurring between 6am and noon on July 20th and 21st when the wind angle is at 160º, but there is a shift in wind direction (190º) on the 22nd when we do not see the peak at the same time.
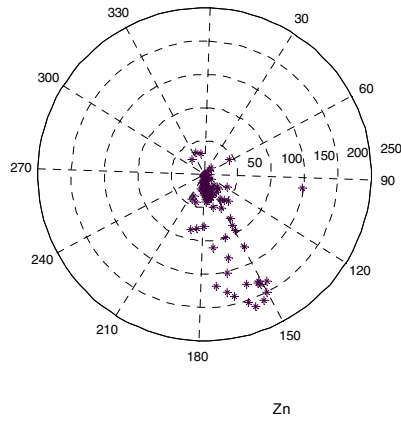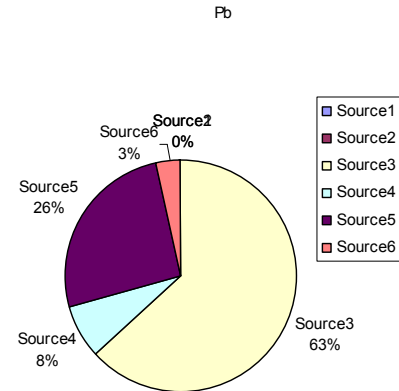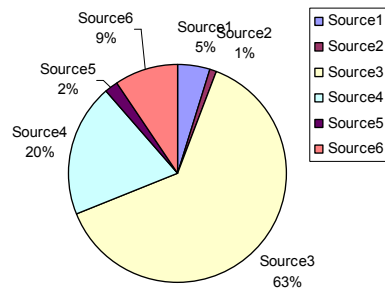
a

b

c

Zn

d

Pb
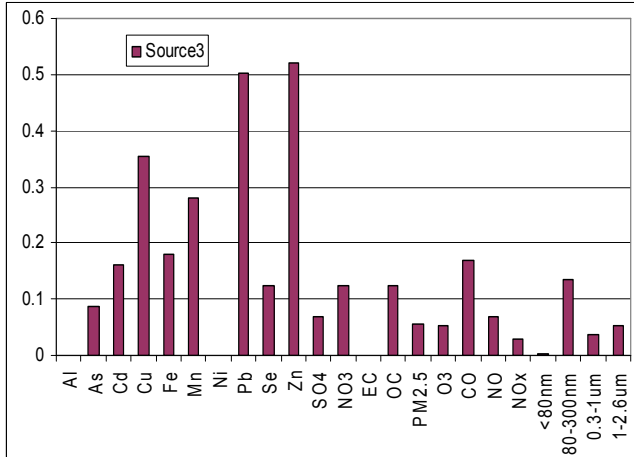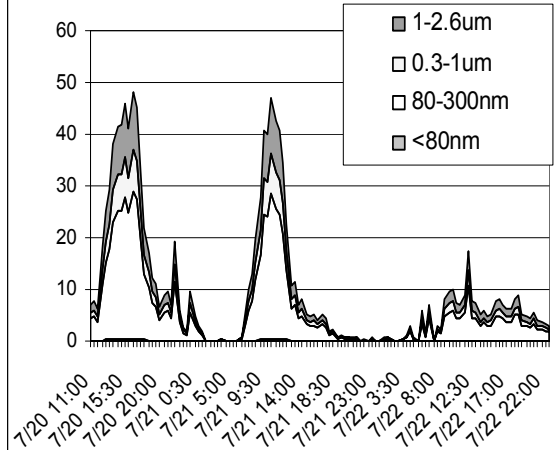
e

6. **Diesel**

Elemental carbon is a tracer for diesel emissions. From the factor loading plotted in Figure XV(b) we see a significant loading of EC contributing to this factor. The EC time series data (Figure V) correlates with the G factor score shown in Figure XV(c) where we see peaks occurring at 21:30 on July 20th, 23:30 on July 20th, 1:00 on July 21st, 5:00 on July 22nd, and 14:30 on July 22nd. Motor vehicle emission peaks are often much broader than industrial source peaks which we see in the G factor score. The nighttime peaks are not surprising since truck drivers often drive at night to avoid traffic backups on I95.

We also know that OC, NO_3 and Fe are tracers for diesel emissions. The source loading (Figure XV(b)) shows a large contribution from Fe, OC and NO_3.

Diesel trucks are uncontrolled combustion sources; therefore they are expected to emit particles in the nucleation particle size mode. We can see from Figure XV(b) that this is in fact the case for this factor.

We can also see from the wind plot shown in Figure XV(a) that the emissions associated with this factor are from 50° and anywhere between 120° and 195°. There is a bus maintenance facility located directly across the street which could be responsible for a fraction of the diesel emissions.

Figure XV. Diesel source profile from Dataset A Figure XV(a) is the directionality plot for diesel emissions while Figure XV(b) is the contribution loading on the source. Figure XV(c) is the G factor and size distribution plot for this factor.

a

b

c
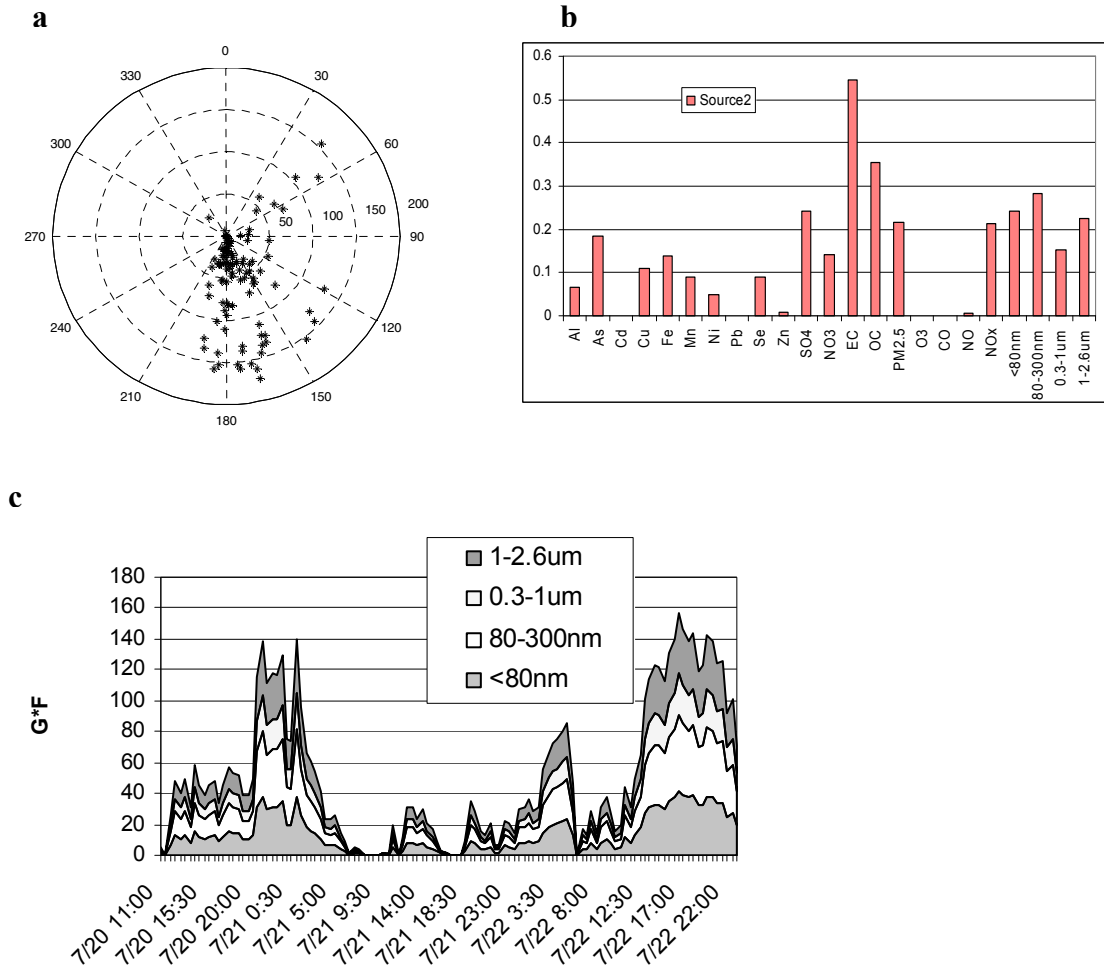
7. Oil-fired power plant

Vanadium and nickel are tracers for oil-fired power plants and refineries (Olmez et al., 1985). Vanadium was not measured in this study; however, nickel is correlates with factor 3 as shown in Figure XVI(a) and the time series analysis, leading us to believe that this factor is an oil-fired power plant. We see that 39% of the Ni is loaded on this factor from Figure XVI(b). The wind angle is from 180-190º

at a speed of 3-5m/s during the peak hours as shown in Figure XVI(c). H.A. Wagner,

a coal/oil/gas-fired power plant is located in the same angular direction as the

Brandon Shores coal-fired power plant (170º). This shows the resolving power of the

model by separating the two factors. It was surprising that more Se was not loaded

on this factor because Brandon Shores is located so close. The particle distribution is

driven by ultra-fine and fresh combustion particles.

Figure XVI. Oil fired power plant. Ni, a tracer for oil-combustion, is shown to contribute 36% to this factor (b). Also, the size distribution plot correlates with this hypothesis, showing that the majority of the particles are from nucleation or fresh combustion sources (a). The source profile shows a nickel peak correlating with the ultra-fine particles as well (d). The wind direction plot shown in figure c looks similar to the wind direction plot for the coal-fired power plant, which is what we would expect.
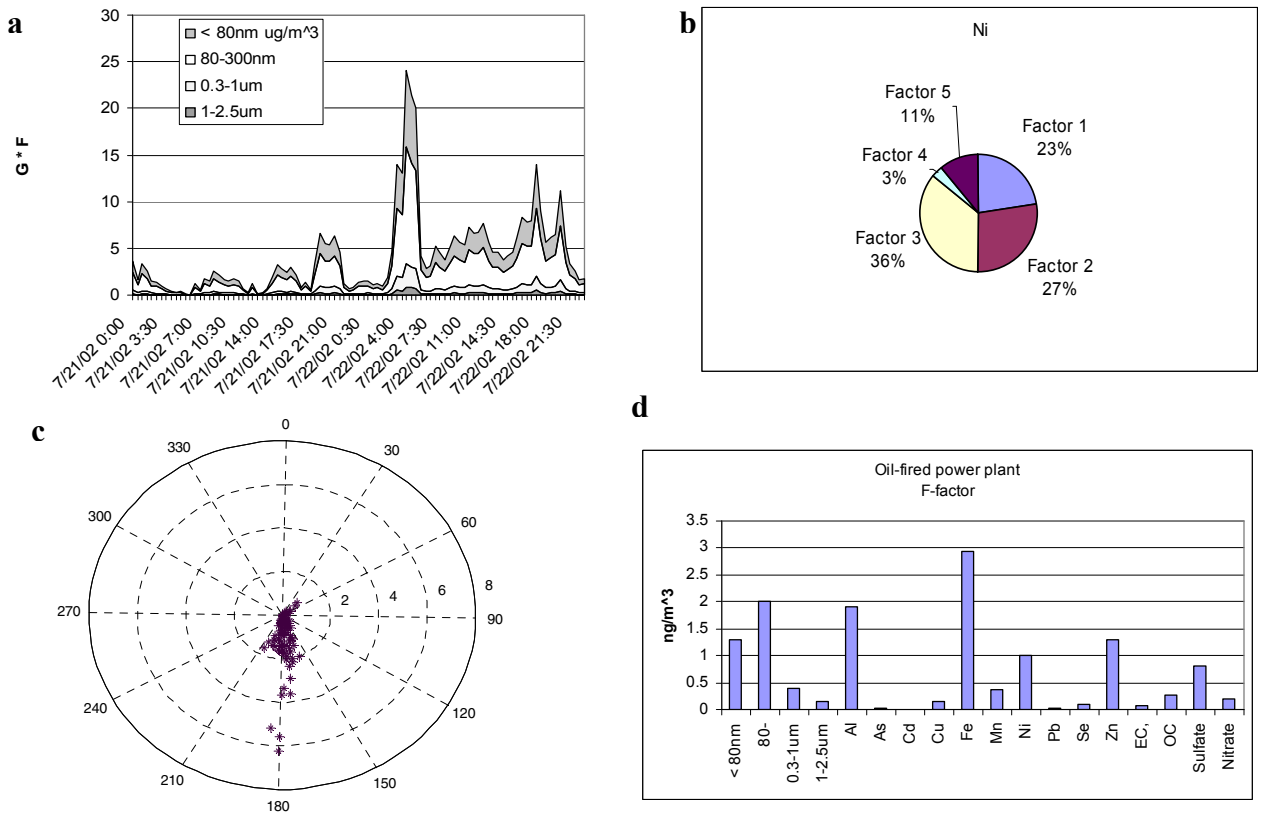
8. Gas-fired power plant

The directionality plot for factor 8 (Figure XVII(a)) shows that the source is located between 120° and 180° with the strongest contribution from the direction of 180°. There is not a large contribution from Se, therefore we do not consider this a plume from Brandon Shores. From the source loading (Figure XVII(b) we see that there is a high concentration of NO and NOx loaded on this factor which could indicate that it is from traffic or gasoline. However, from the G factor score we see that this factor has only one large peak at 4:30 on July 22nd. Typically traffic peaks diurnally and the peaks are broad. There is a gas power generator at H.A. Wagner that could have been turned on for a few hours in the morning of the 22nd which would give us a peak in NO and NO_x emissions. H.A. Wagner is located at 170° and it is reasonable to assume that they would not use the gas generator daily due to cost.

The size distribution graph (XVII(c)) convincingly shows that this source is from a source emitting mostly fresh nuclei particles. It is probable that the gas-fired power plant is an uncontrolled combustion source creating a plume containing particles in the <80 nm size range.

Figure XVII. Gas-fired power plant factor from Dataset A. Figure XVII(a) is the directionality plot showing the source is located between 120° and 180°. Figure XVII(c) shows there is one large peak at 4:30 on July 22nd. From the size distribution graph we can see that most of the particles are loaded in the <80 nm size range indicating the source is emitting particles in the nucleation mode.

a

b

c
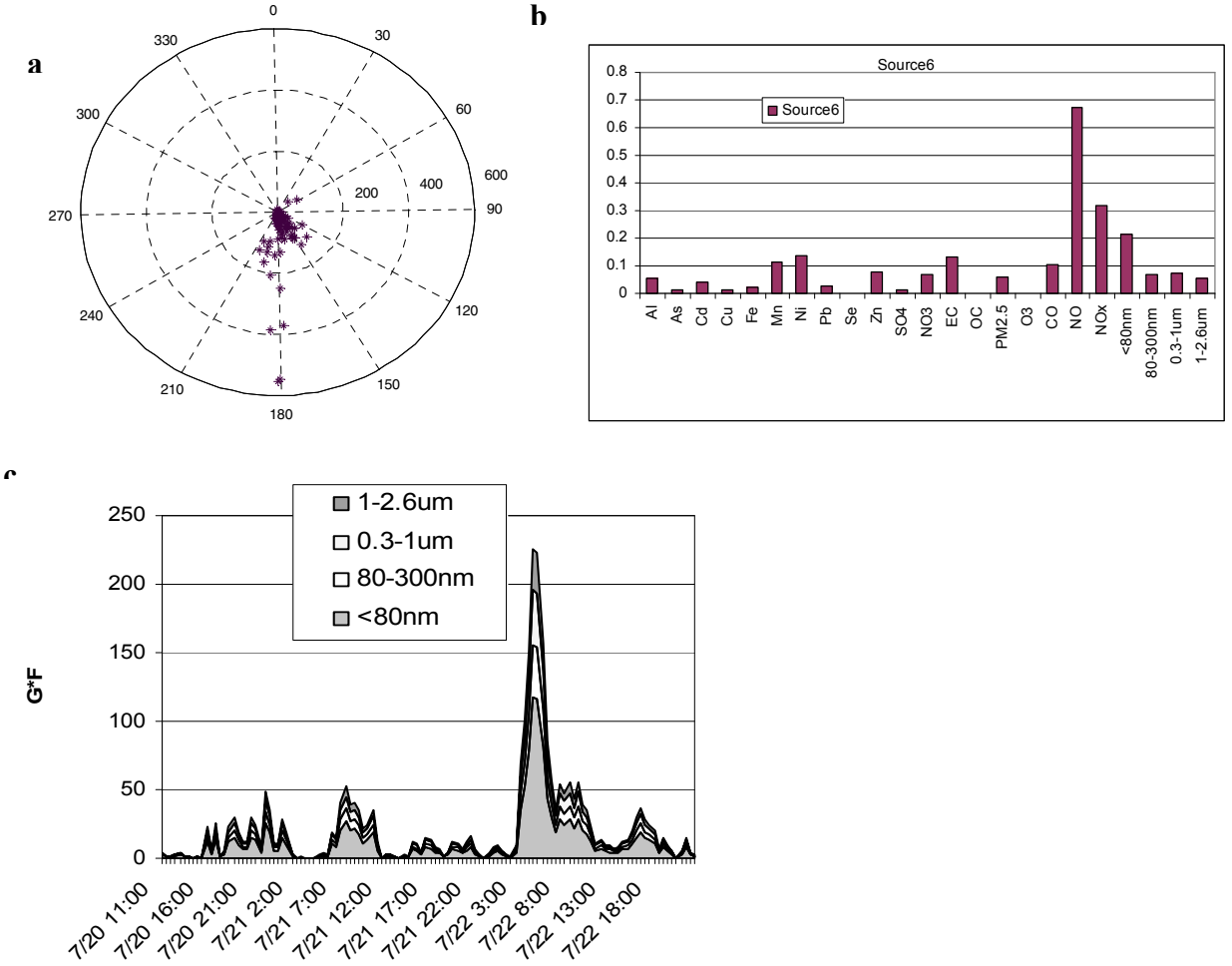
Chapter 4: Conclusions

A. Conclusions

A total of eight emissions sources have been identified over a two day period in July 2002 using four discrete particle size bins and positive matrix factorization. Nucleation mode (< 80 nm), fresh combustion (80-300 nm), secondary or transported aerosol (0.3-1μm), and dust or aged aerosol (1-2.5μ) size bins were created to identify the type (controlled vs uncontrolled combustion) and age (transported or secondary vs local or primary) of the particles partitioned into source profiles by PMF.

From an initial metals, gases, EC/OC concentration time series data analysis we determined that we would likely see at least 5 sources. There were five selenium peaks which were very obviously from the Brandon Shores coal-fired power plant located at 170°. We saw a Ni peak also at the time when the wind direction was from 170° where H.A. Wagner oil-fired power plant is located. We were also able to identify an incinerator peak by Cd:Zn and Pb:Zn concentration ratios. We expected to see a traffic source with particle counts or particle mass loaded in the nucleation size bin and a nitrate event occurring during the daylight hours when ozone levels were low. and a Five fine particle emissions sources have been identified by concentration and size distribution data collected at the Baltimore Supersite using multivariate factorization modeling techniques. Elemental tracers from various sources have been used to apportion sources for decades by statistical modeling. Improvements have been made in this analysis by using particle sizes to look more closely into the location and types of emissions sources. We have shown that discrete size bins can be used to differentiate fresh combustion particles from aged aerosol.

Particle mass is used for pollution control legislation developed by the EPA, however, it is the submicron particles which are the most toxic to humans. Nucleation and fresh combustion particles do not contribute significant amounts to particle mass due to their physical size. First we found that by using particle counts in discrete size bins created heavy loadings in the nucleation and fresh combustion size bins, where we would expect the greatest number of particles, but few particles fell into the two upper size bins. Calculating mass concentrations of particles created a matrix of concentrations for all data points, while using number counts gave results which had mixed units.

This work can be used to show the atmospheric particle mass concentrations associated with power generation emission sources such as coal- and oil-fired power plants. We have found that coal-fired power plant emissions from Brandon Shore contributed to more than 90% of the Se concentration in Baltimore, which agreed with a study by Kowalczyk et al. (1982). We also found that the ratio of As/Fe from a steel plant is 0.0037 compared with a previous study which reported the ratio as 0.0011 (Small, 1979).

Source apportionment results that show significant particle counts associated with the nucleation mode may lead to stricter regulations on fine particle emissions directed at the largest contributors. Also, the EPA could use these models to make a case for alternative energy sources such as wind or hydro-power generation which contribute little to the atmospheric particle emissions.

B. Future Improvements

In the future more extensive time periods should be employed. This analysis was done using a two-day time period when sources were thought to be limited, so we could focus on time series peaks and the PMF factor results. From the Baltimore Supersite alone, there are 11 months of data that can be analyzed by PMF using mass and elemental concentrations.

The analysis time for the SEAS samples by graphite furnace AA takes up to six hours for 11 elements. In the future ion coupled plasma mass spectrometry can be used. The ICP-MS will detect more elements with much faster analysis times. This will improve the results by measuring elements such as vanadium, a marker for oil combustion, and titanium, a tracer of paint manufacturers.

From this study we have learned that PMF is not the best model because it does not find unique sources. PMF will bin common sources into one factor and then the modeler will need to plot wind direction data to identify the sources. The model can be improved by using the pseudo-deterministic receptor model (PDRM) created by Park et al (2005). The PDRM is a Gaussian plume dispersion model which utilizes stack heights, wind directions and wind speeds to identify emissions sources.

Bibliography

Divita, F., Ondov, J.M., Suarez, A.E., 1996. Size Spectra and atmospheric growth of V-containing aerosol in Washington DC. Aerosol Science and Technology 25, 256-273.

Dockery, D.W., Pope, C.A., Xu, X., Spengler J.D., Ware, J.H., Fay, M.E., Ferris, B.G., Speizer, F.E., 1993. An Association between Air Pollution and Morality in Six US Cities. The New England Journal of Medicine 329, 1753-1759.

Dodd, J.A., Ondov, J.M., Tuncel, G., 1991. Multimodal size spectra of submicrometer particles bearing various elements in rural air. Environmental Science & Technology 25, 890-903.

Environmental Progress Report (2004) Constellation Energy http://www.constellationenergy.com/about/environreport_2004.pdf.

Gordon, Glen E. 1988. Receptor Models. Environmental Science and Technology 22, 1132-1142.

Greenberg, R.R., Zoller, W.H., Bordon, G.E., 1978. Composition and size distribution of particles released in refuse incinerators. Environmental Science & Technology 12, 566-573.

Harrison, D., Park, S.S., Ondov, J., Buckley, T., Kim, S.R., Jayanty, R.K.M. (2004) Highly time resolved fine particle nitrate measurements at the Baltimore supersite. Atmospheric Environment 38, 5321-5332.

Harrison, D. et al. (2003) Highly-time resolved particulate sulfate measurements at the Baltimore Supersite, in prep. 2003.

Hazi, Y., Heikkinen, M.S.A., Cohen, B.S., 2003. Size Distribution of Acidic Sulfate Ions in Fine Ambient Particulate Matter and Assessment of Source Region Effect. Atmospheric Environment 37, 5403-5413.

Henry, R., 1997. History and fundamentals of multivariate air quality receptor models. Chemometrics and Intelligent Laboratory Systems 37, 37-42.

Henry, R., 2000. UNMIX theory and applications. In: Willis, R.D. (Ed.), Final Report Workshop of UNMIX and PMF as Applied to $PM_{2.5}$. United States Environmental Protection Agency, Washington, EPA/600/A-00/48.

Henry, R.C., Park, E.S., Spiegelman, C.H., 1999. Comparing a new algorithm with the classical methods for estimating the number of factors. Chemom. Intell. Lab. Syst. 48, 91-97.

Hinds, W.C.: Aerosol Technology: Properties, Behavior, and Measurement of Airborne Particles. New York, John Wiley & Sons, 1999.

Junge, C. E., 1954. The chemical composition of atmospheric aerosols, I. Measurements at Round Hill Field Station, June-July 1953. Journal of Meteorology 11, 323-333.

Kidwell C.B., Ondov, J.M., 2001. Development and evaluation of a protype system for collecting sub-hourly ambient aerosol for chemical analysis. Aerosol Science and Technology 35, 596-601.

Kidwell, C.B., Ondov, J.M, 2004. Elemental Analysis of sub-hourly ambient aerosol collections. Aerosol Science and Technology 38, 205-218.

Kidwell, C.B., Divita, F., Ondov, J.M., 1996. Identifcation of an incinerator plume from ground-level submicrometer aerosol sampling with a micro-orifice impactor. *J. Aerosol Sci. 27,* S29-S30.

Kowalczyk, G.S., Gordon, G.E., Rheingrover, S.W., 1982. Identification of atmospheric particulate sources in Washington, D.C. using chemical element balances. Environmental Science & Technology 16, 79-90.

Law, S.; Gordon, G.E., 1979. Sources of metals in municipal incinerator emissions. Environmental Science & Technology 13, 432-438.

Lee, J.H., Hopke, P.K., Holsen, T.M., Polissar, A.V., Lee. D., Edgerton, E.S., Ondov, J.M., Allen, G., 2005. Measurements of fine particle mass concentrations using continuous and integrated monitors in Easter US cities. Aerosol Science & Technology 39, 261-275.

Maciejczyk, P.B., 2000. Atmospheric fate and dry deposition fluxes of particles bearing trace elements and soot in the Baltimore area. Ph.D. Thesis, University of Maryland, College Park.

Manoli, E., Voutsa, D., Samara, C., 2002. Chemical Characterization and Source Identification/Apportionment of Fine and Coarse Air Particles in Thessaloniki, Greece. Atmospheric Environment 36, 949-961.

Markowski, G.R., Ensor, D.S., Hooper, R.G., Carr, R.C., 1980. A submicron aerosol mode in flue gas from a pulverized coal utility boiler. Environmental Science & Technology 14, 1400-1402.

Mroz, E.J., 1976. The study of elemental composition of particulate emissions from an oil-fired power plant. Ph.D. Thesis, University of Maryland, College Park.

Ogulei, D. Hopke, P.K., Zhou, L., Paatero, P., Park, S.S., Ondov, J.M., 2005. Receptor modeling for multiple time resolved species: The Baltimore supersite. Atmospheric Environment 39, 3751-3762.

Olmez, L., Gordon, G.E., 1985. Rare earths: Atmospheric Signitures for oil-fired power plants and refineries. Science 229, 966-968.

Ondov, J.M., Kelly, W.R., Holland, J.Z., Lin, Z., Wight, S.A. (1992) Atmospheric Environment 26B, 453-462.

Ondov, John M., Wexler, Anthony S., 1998. Where Do Particle Toxins Reside? An Improved Paradigm for the Structure and Dynamics of the Urban Mid-Atlantic Aerosol. Environmental Science & Technology 32, 2547-2555.

Ondov, J.M., Buckley, T.J., Hopke, P.K., Parlange, M.B., Rogge, W.F., Squibb, K.S., Wexler, A.S., 2004. Baltimore Supersite: highly time and size resolved concentrations of urban $PM_{2.5}$ and its constituents for resolution of sources and immune responses. 15th Quarterly Report Summary, Jan. 2004. http://www.epa.gov/ttnamti1/files/ambient/super/blt15.pdf.

Paatero, P. (1997) Least-squares formulation of robust non-negative factor analysis. *Chemom. Intell. Lab. Sys.* 37, 23-35.

Paatero, P., Tapper, U. (1994) Positive matrix factorization-a non-negative factor model with optimal utilization of error estimates of data values. *Environmetrics* 5, 111-126.

Pancreas, J.P., Ondov, J.M., Zeisler, R., 2005. Multielement electrothermal AAS determination of 11 marker elements in fine ambient aerosol slurry samples collected with SEAS-II. Analytica Chimica Acta 538, 303-312.

Pancras, J.P., Ondov, J.M., Poor, N., Landis, M.S., Stevens, R.K, 2006. Identification of sources and estimation of emission profiles from highly time-resolved pollutant measurements in Tampa, FL. Atmospheric Environment (*in press*).

Park, Seung S., Kim, Young J., 2004. $PM_{2.5}$ Particles and Size-Segregated Ionic Species Measured During Fall Season in Three Urban Sites in Korea. Atmospheric Environment 38, 1459-1471.

Park, S.S. Kleissl, J., Harrison, D., Nair, N.P., Kumar, V., Ondov, J., 2005. Highly time-resolved organic and elemental carbon measurements at the Baltimore supersite at Ponca St. Journal of Geophysical Research-Atmospheres 110.

Park., S.S., Pancras, J.P., Ondov, J.M., Poor, N., 2005. A new-pseudo-deterministic multivariate receptor model for accurate individual source apportionment using highly time-resolved ambient concentrations. Journal of Geophysical Research 110

Park, S.S., Kleissl, J., Harrison, D., Nair, N.P., Kumar, V., Ondov, J.M., 2006 (expected) Investigation of $PM_{2.5}$ episodes using semi-continuous instruments at the Baltimore supersite at Ponca St.

Rodhe, H., Grandell, J., 1981. Estimates for Characteristic Times for Precipitation Scavenging. Journal of the Atmospheric Sciences 38, 370-386.

Schauer, J.J., Rogge, W.F., Hildemann, L.M., Mazurek, M.A., Cass, G.R., 1996. Source apportionment of airborne particulate matter using organic compounds as tracers. Atmospheric Environment 30, 3837-3855.

Seinfeld J.H., Pandis, S.N.: Atmospheric Chemistry & Physics, New York, Wiley, 1988.

Shrock, J., Bowser, J., Mayhew, W., Stevens, R.K., 2002. South Florida mercury monitoring and modeling pilot study. EPA report 600/R-00/102.

Song, X., Polissar, A.V., Hopke, P.K., 2001. Source of Fine Particle Composition in the Northeastern US. Atmospheric Environment 35, 5277-5286.

Stolzenburg, M., Hering, S.V., 2000. Method for the automated measurement of fine particluate nitrate in the atmosphere. Environmental Science & Technology 34, 907-914.

Suarez, A. E., Ondov, J.M., 2002. Ambient Aerosol Concentration of Elements Resolved by Size and by Source: Contributions of Some Cytokine-Active Metals from Coal- and Oil-Fired Power Plants. Energy Fuels 16, 562-568.

Warneck, P.: Chemistry of the Natural Atmosphere, Academic Press, San Diego, 1988.

Watson, J.G., Chow, J.C., Pace, T.G., 1991. Chemical mass balance. Receptor Modeling for Air Quality Management 7, 83-116.

Watson, J.G., Chow, J.C., Lu, Z.Q., Fujita, E.M., Lowenthal, D.H., Lawson, D.R., Ashbaugh, L.L., 1994. Chemical mass-balance source apportionment of PM(10) during the southern California air-quality study. Aerosol Science and Technology 21, 1-36.

Webber, R., Orsini, D., Duan, Y., Baumann, K., Kiang, C.S., Chameides, W., Lee, Y.N., Brechtel, F., Klotz, P., Jongejan, P., Brink, H., Slanina, J., Boring, C.B., Genfa, Z., Dagupta, P., Hering, S., Stolzenburg, M., Dutcher, D.D., Edgerton, E., Hartsell,

B., Solomon, P., Tanner, R., 2003. Intercomparison of near real-time monitors of PM$_{2.5}$ nitrate and sulfate at the EPA Atlanta supersite. Geophysical Research 108, 8421-8433.

Whitby, K.T., 1978. Physical Characteristics of sulfur aerosols. Atmospheric Environment 12, 135-159.

Zhou, Liming, Kim, Eugene, Hopke, Philip K., Stanier, Charles O., 2004. Advanced Factor Analysis on Pittsburg Particle Size Distribution Data. Aerosol Science and Technology 38(S1), 118-132.